Title:

Towards an in-situ evaluation methodology of thermal resistance of basement walls in buildings

Authors:

David Bienvenido-Huertas[1]*, Juan Luis Pérez-Ordóñez[2], Juan Moyano[1], Sindy Seara-Paz[2]

[1] Department of Graphical Expression and Building Engineering, University of Seville, 41012 Seville, Spain.

[2] Department of Civil Engineering, University of A Coruña, E.T.S.I. Caminos, Canales, y Puertos. Campus Elviña s/n, 15071 A Coruña, Spain.

*Author to whom correspondence should be addressed;

Higher Technical School of Building Engineering, Ave. Reina Mercedes 4A, Seville, Spain

E-Mail: jbienvenido@us.es (D.B.H.); Tel.: +34-954556626

Highlights:

- Proposal of a methodology to analyse the thermal resistance of basement walls.
- The design of a calibrated hot-box for samples in contact with the ground.
- Analysis of three regression algorithms.
- Accurate estimations using monitored data of 2 days.
- Validation in actual case studies.

Abstract:

One of the essential aspects in building energy analysis is determining correctly the thermal characteristics of envelopes. Characterizing envelope elements accurately allows energy consumption to be predicted and energy saving measures to be established. Basement walls are among those common envelope elements in buildings. The estimation of their thermal resistance is a challenge due to the difficulties and the lack of methodologies to know the wall stratigraphy. This study establishes a methodology to characterize the thermal resistance of this kind of walls. Such methodology consists in monitoring easily measurable variables (internal air temperature, external air temperature, ground temperature, internal surface temperature, and heat flux) which, together with the use of regression models, estimate thermal resistance. The methodology is validated in 2 phases: (i) in a calibrated hot-box adapted to elements in contact with the ground, and (ii) by analysing actual case studies. With the data obtained, various regression models are created based on time windows. The M5 Prime algorithm with a time window of 2 days of observation made accurate estimations in the case studies. An efficient methodology is therefore developed for estimating the thermal resistance in actual case studies. Also, the calibrated hot-box adapted could be used to analyse samples under controlled conditions in laboratory.

Keywords:

Thermal resistance; basement walls; regression algorithm; calibrated hot-box.

Nomenclature

Symbols

MAE	Mean absolute error
n	Number of instances in the dataset
q_j	Heat flux
$\overline{q}$	Heat flux average
R^2	Coefficient of determination
$RMSE$	Root mean square error
s_i	Thickness of the i layer of the wall
t_i	Actual value
T	Number of tree models
$T_{s,in,j}$	Internal surface temperature
$T_{s,out,j}$	External surface temperature
$\overline{T}_{external}$	Average of the external air temperature
$\overline{T}_{ground}$	Average of the ground temperature
$\overline{T}_{internal}$	Average of the internal air temperature
$\overline{T}_{surface-internal}$	Average of the internal surface temperature of the basement wall
TR	Thermal resistance of the wall
$TR_{\text{Estimated}}$	Thermal resistance of the wall estimated by regression models
$TR_{\text{Reference}}$	Thermal resistance of the wall calculated according to ISO 6946
v_i	Independent variables

$w_{ji}^{(1)}$	Weights of the hidden layer
$w_{kj}^{(2)}$	Weights of the output layer
$w_{k0}^{(2)}$	Weights of the bias neuron of the hidden layer
x_i	Values of the input layer
y_0	Input value of the bias neuron of the hidden layer
$\hat{Y}_{MLP}$	Output value of the multilayer perceptron
$\hat{Y}_{RF}$	Output value of random forest
$\hat{Y}_t$	Output of the t-th tree
Greek letters	
β_0	Independent term
β_i	Regression coefficients
ε	Error
λ_i	Thermal conductivity of the i layer of the wall
σ	Activation function
Abbreviations	
CHB	Calibrated hot-box
FEM	Finite Element Method
M5P	M5 Prime
MLP	Multilayer perceptron
MLR	Multiple linear regression
RF	Random forest

1. Introduction

The high energy consumption of residential buildings is nowadays one of the main international problems, constituting 40% of the total energy consumption in the European Union member countries [1,2]. Such percentage is very similar to that of carbon dioxide emissions (36%) [3,4]. Although the energy is consumed by various elements (e.g., electrical household appliances and lighting), the highest energy consumption is attributed to air conditioning systems [5]. Other aspects emerging in recent years, such as fuel poverty [6] and the increase of deaths for not having acceptable thermal comfort conditions [7], have raised the awareness of the energy problem in buildings. Consequently, national and international policies have been developed to resolve that situation. The European Union has established objectives to be achieved by 2050 and aimed at significantly decreasing the greenhouse gases emitted to the atmosphere [8]. The main pollutant sectors should achieve percentage reductions of their emissions compared with the levels from 1990. Regarding the building sector, emissions should be reduced by 90%. For this purpose, the roadmap sets up the need of improving the existing building stock.

Buildings having inhabitable rooms in contact with the ground should be analysed. The advantage of having rooms with elements in contact with the ground is to be able to reduce the variations of internal temperatures [9,10]. In this sense, Carmody and Steerling [11] indicated that the ground temperature in summer days do not reach the external temperature values so that the thermal differential is reduced. Other advantages are that appropriate conditions are met to store food [12] and noise immissions are reduced [13]. As a consequence, they have been frequently used as a design technique in buildings since the beginning of mankind . Also, their energy performance, such earth shelter dwellings [14] and caves [15], have been analysed. Although such constructions allow thermal oscillations to be reduced, the heat transfers through elements in contact with the ground can be high, even being responsible for 50% of the total energy consumed [9,16]. The establishment of adequate designs or the improvement of these envelopes would therefore keep an acceptable thermal comfort in internal rooms [17] and reduce the energy consumption, thus being an effective option to obtain zero-energy buildings [18].

Many research works are focused on the influence of thermal properties of envelopes on building energy consumption: Aksoy and Inalli [19] studied how heating insulation affected a building located in a cold climate zone, resulting in obtaining heating energy saving rates from 34% to 36%; (ii) Invidiata et al. [20] analysed the influence of six design strategies on a building in future scenarios of climate change using the morphing process. The results indicated that the design of sustainable envelopes could ensure a lower energy consumption in 2050 and 2080; (iii) Bhikhoo et al. [21] carried out a sensibility analysis in various design aspects of envelopes of typical dwellings in Thailand. The results reflected how placing an insulating material at the ceiling affected the energy consumption; (iv) Ge et al. [22] analyzed several measures to reduce the energy consumption in university buildings. The improvement in the thermal performance of the envelope influenced the energy consumption in all seasons; (v) Yuan et al. [23] analysed the influence of the characteristics of insulation materials on the envelope. The location of the insulation had different results. In this sense, rooms with external insulation had an energy consumption lower than rooms with internal insulation (the percentage deviation was higher than 18%); (vi) in a study by Ramalho de Freitas and Grala da Cunha [24], the impact of thermal bridges of reinforced concrete structures on the energy performance of a building was analysed, proving that

the energy consumption can vary up to 20%; and (vii) Ge et al. [25] studied the influence of thermal bridges caused through the balconies on residential buildings. The results showed an influence of 1% on the cooling energy consumption, and between 5 and 13% on the heating energy consumption.

The thermal resistance of envelopes is among those variables defining its thermal properties which most affect the energy performance [26,27] because it reduces heat gains or losses with the exterior, thus varying the energy consumption of HVAC systems [28–30]. The increase of the thermal resistance of the envelope is therefore one of the most possible measures to be used in order to reduce the heat transfer with the exterior and, in turn, the energy consumption [31].

Characterizing correctly the thermal resistance of envelopes is fundamental in energy audit works because the thermal resistance values of the envelope are generally underestimated, thus overestimating the building energy demand [32,33]. By defining correctly the thermophysical properties of the envelope, energy simulations can also be performed with various energy conservation measures to determine which is the most adequate [34]. A mistaken estimation of thermal resistance can simply not improving the most deficient envelope elements [35] or increase the economic amortization periods of the measures to be adopted [36].

Thermal resistance can be determined by various methods, both manual calculations or in-situ measurement procedures. The main difference between both typologies is the lower associated error that experimental methods generally have [37].

The manual calculation method is included in the ISO 6946 standard [38]. In such standard, the thermal resistance is determined by the sum of the thermal resistance of each layer of the wall, which is obtained by its thickness and thermal conductivity. It is a procedure limited used in energy audits because the composition and characteristics of the layers of the wall are generally unknown. Among the various techniques for determining the composition of walls, the endoscopic analysis [39] and the use of reliable technical documentation [40] are the most acceptable techniques. However, their use can be limited due to both the damages generated in the wall by using the endoscopic analysis and the lack of technical documentation of old buildings [37]. In addition, thermal conductivity values are usually obtained from technical documents or catalogues in which ranges of possible values for a same material are indicated. The results of thermal resistance can therefore be quite different [37]. So, some studies analyse the uncertainty of values obtained with this methodology [39]. Also, another aspect causing a high uncertainty when estimating the thermal resistance can be moisture presence [41] or degradation of the thermal properties of layers [42]. Nevertheless, it is a method widely used for designing buildings, justifying the regulations of each country, and validating the results obtained in in-situ measurement methods [37].

Concerning experimental methods, 3 of them widely developed in recent years are considered: the heat flow meter method, the quantitative method through infrared thermography, and the thermometric method. The heat flow meter method is included in ISO 9869-1 [43], the only experimental method having a test standard. Such method consists in obtaining the thermal resistance value by measuring heat flux and surface temperatures. In addition, it greatly influences the heat flux measurement in the error of the result obtained. Cesaratto et al. [44], Desogus et al. [45], and Trethowen [46] stressed the possible disturbance caused by placing the heat flux plate in the heat flux of the wall. Also, the location of the plate in the wall can alter the results, and the maximum error can reach 26% [47]. Ficco et al. [39] developed a long list of the various uncertainty contributions, including the bad contact between the probe and the wall and the influence of interstitial condensations. Furthermore, such method needs specific location and environmental conditions to estimate thermal resistance. High thermal gradients (e.g., greater than 10 ºC) between the interior and exterior obtain more representative results than low thermal gradients [45]. Likewise, vertical walls (e.g., façades) facing north should be analysed because high deviations are not presented in comparison with the other orientations [48].

As a result, two alternatives emerged in recent years: the quantitative method through infrared thermography and the thermometric method. The former is characterized by using an infrared camera to determine convective and radiative heat fluxes of walls [49]. This approach is different from the others because it determines the possible thermal heterogeneities of a wall, thus avoiding the analysis of the areas affected by condensations or damages [37]. Also, there is a wide variety of infrared thermography methods, but the main difference depends on both the location of the camera and the expression used for the convective coefficient. Methods from the interior [50] and the exterior [51] can therefore be distinguished. In addition, stationary and dynamic analysis can be used in this methodology [52]. Regarding the thermometric method, the infrared camera is replaced by surface temperature probes [53]. The main advantage of such methods is replacing the heat flux measurement with other variables to reduce the error associated and operational limitations, although other error sources can appear. Also, deviations in the measurements of temperature and wind speed can affect the results by 50% [47,54]. Moreover, the location and environmental requirements for the heat flow meter method are the same in both methods [55].

All of them are useful to analyse walls in contact with the external air. However, they are not suitable for analysing walls in contact with the ground, so simulation methods by means of finite elements or manual calculations are generally used [56]. The ISO 13370 [57] includes the main methods of calculation of heat transfer coefficients and heat flow rates for building elements in thermal contact with the ground. It applies to building elements, or parts of them, below a horizontal plane in the bounding walls of the building situated at the level of the external ground surface, for heated basements. Nevertheless, determining some parameters (e.g., the thermal resistance of basement walls) through ISO 6946 is required (see Eq. (1)), thus limiting their correct application, as mentioned above. This particularly occurs in the energy audits carried out in buildings whose constructive composition is unknown. The energy simulations of this kind

of buildings could obtain non-representative results and the proposed energy conservation measures could be inadequate, thus making the fulfilment of the objective for 2050 something of a challenge.

$$U_{wg;b} = \frac{2 \cdot \lambda_g}{\pi \cdot z} \cdot \left(1 + \frac{0.5 \cdot d_f}{d_f + z}\right) \cdot \ln\left(\frac{z}{\lambda_g \cdot (R_{si} + R_{w;b} + R_{se})}\right) \quad (1)$$

Where $R_{w;b}$ is the thermal resistance of the basement wall [(m²K)/W], λ_g is the thermal conductivity of the ground [W/(mK)], d_f is the total equivalent thickness [m], and z is the depth of the basement floor below fround level [m].

This study therefore suggests a methodology to assess the thermal resistance of basement walls. Such methodology consists in measuring the ground temperature, the surface temperature and the heat flux of a basement wall, and the internal and external air temperatures. Regarding data, various regression algorithms were used to determine the most adequate to analyse them. To establish the methodology, the feasibility of the method was analysed in a hot-box design for elements in contact with the ground. Afterwards, and based on the results obtained in the laboratory test, two actual case studies were analysed. The regression models were previously trained by using a sampling of 10,579 tests simulated by means of the Finite Element Method (FEM). After generating such models, the accuracy of the estimations of the thermal resistance of both case studies was analysed with the reference values.

The importance of this study lies in the lack of methods analysing the thermal resistance of basement walls through in-situ measurements, as most studies focus on walls in contact with the air. Such lack of methods makes the energy assessment in buildings with such envelope something of a challenge. The elements of an envelope influence the energy consumption of buildings, and methods assessing their thermal behaviour are required. In this sense, some studies showed the possible deviations in the determination of the thermal properties of the envelope: (i) Rotilio et al. [58] assessed 4 walls in Italian historic buildings with the heat flow meter method. The results reflected deviations of up to 15% between the value obtained by the heat flow meter method and the value calculated according to the Italian energy regulation for buildings; and (ii) these deviations between tabulated procedures and in situ methods were also reflected by Lucchi [59,60], who monitored historical stone and brick walls. The results showed deviations between the measured values and the values tabulated and calculated according to the Italian energy regulation for buildings.

Moreover, there is a knowledge gap with respect to methods assessing the thermal resistance in basement walls, their influence on the energy performance of buildings, and the most adequate energy conservation measures. This study proposes therefore a methodology to assess the thermal resistance in basement walls. More research studies could be conducted with such methodology, as well as the energy efficient could be analysed in this kind of buildings. The use of regression algorithms, such as multilayer perceptrons or random forests, constitutes a new aspect in the analysis of thermal behaviour of building envelopes. There are nowadays few articles analysing the use of advanced algorithms in thermal characterization problems. Although neural network algorithms were used [61,62], tree algorithms have only been used to estimate the thermal transmittance of ISO 6946 in enclosures in façades [63]. Also, it is the first time that a test is previously conducted in laboratory using a hot-box adapted to elements in contact with the ground. The main contributions of this study are as follows:

- Design of a specific hot-box to characterize the thermal behaviour of samples in contact with the ground. Hot box has been used as a method for evaluation of thermal properties of building elements, such as: (i) Prata et al. [64], studied the thermal behaviour of a thermal bridge in a wooden building corner; (ii) Jeong et al. [65] have also used hot box to evaluate the thermal properties of large-scale thermally-enhanced concrete specimens; and (iii) Kus et al. [66] evaluated the hygrothermal performance of a pumice aggregate concrete hollow blocks wall using a hot box. Nevertheless, hot box has never been used to assess thermal properties of samples in contact with the ground.
- Development of a methodology with regression algorithms to assess the thermal resistance of samples in contact with the ground by using the data obtained through the hot-box tests.
- Development of a methodology to determine the thermal resistance in actual basement walls through data obtained in FEM simulations and using regression algorithm. The methodology was validated in actual case studies.

An adequate methodology could be provided with the main contributions of this paper to analyse buildings with inhabitable rooms in contact with the ground, thereby guaranteeing a high energy analysis rate and establishing energy conservation measures to reduce energy consumption. In addition, the evaluation of the thermal resistance of basement walls would allow a better use of ISO 13370 and it would facilitate the analysis of compliance in those countries that establish limitations in the thermal properties of basement walls (e.g., Spain through the Spanish Building Technical Code [67]). As a result, the objectives set up by the European Union for a low-carbon economy would be achieved [8], thus reducing the environment pollution and the impact of the predicted future scenarios of climate change [6].

This paper starts by describing the methodology in Section 2, which is in turn divided into subsections as follows: (i) regression algorithms used and training and validation procedure of the regression models; (ii) test in a hot-box; (iii) test in buildings; and (iv) two-dimensional simulations. Section 3 analyses the results obtained in the first phase of the tests using the hot-box. Afterwards, the results obtained in the second phase corresponding to the practice application of the analysis methodology in actual case studies are discussed. Finally, Section 4 includes the main conclusions.

2. Methodology

This paper focuses on establishing a methodology to estimate in-situ the thermal resistance of basement walls. Firstly, the feasibility of using the methodological approach was analysed under controlled conditions. Then, various data analysis models were developed by using simulation data to be applied in actual case studies. Figure 1 sums up the flowchart of this research, which is developed in the following subsections.

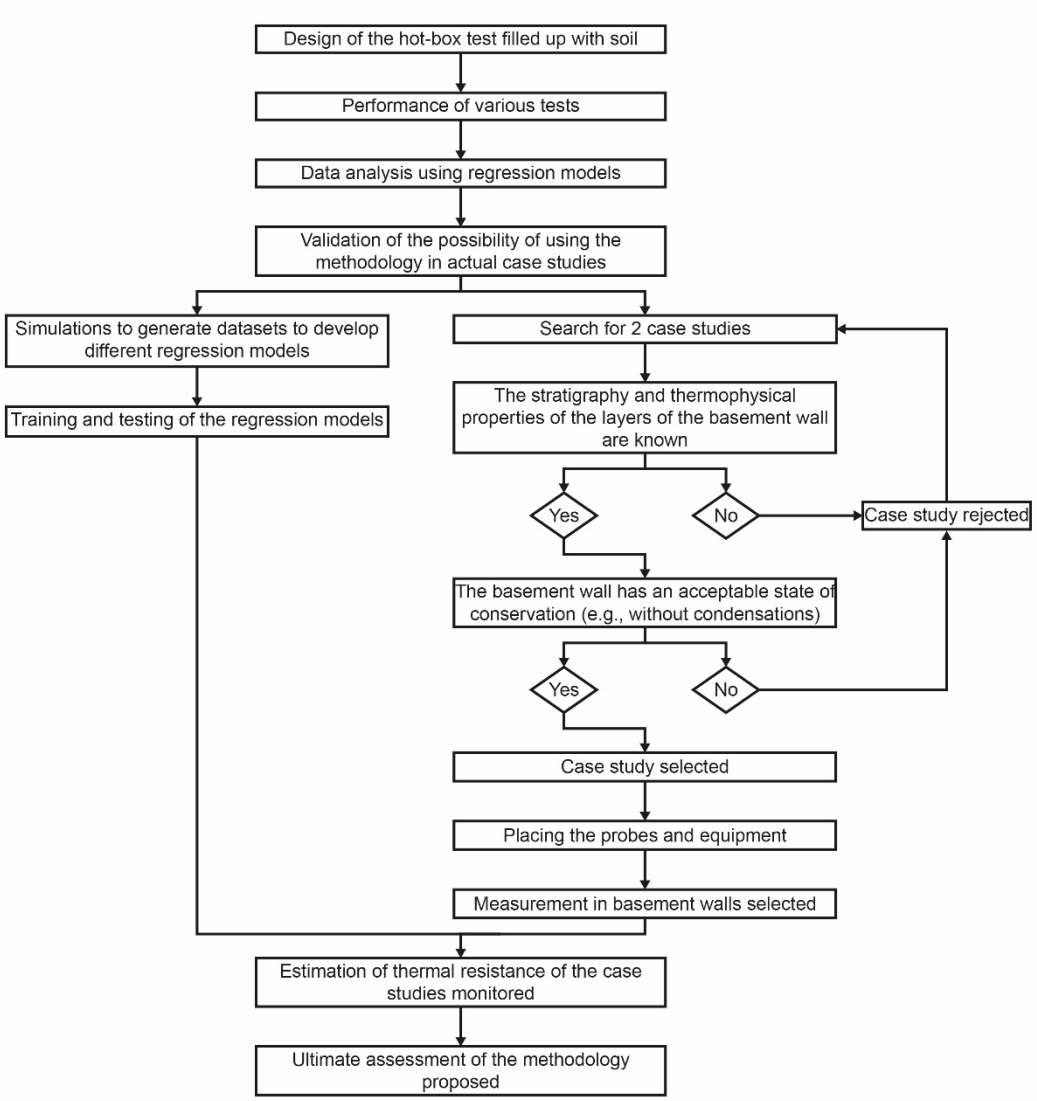

Figure 1. Flowchart with the steps of this research.

2.1. Theory

As indicated above, the thermal resistance of an element (whose reciprocal is its thermal conductance) can be obtained by the sum of the thermal resistances of each layer following the methodology in ISO 6946 (see Eq. (2)).

$$R = \sum_{i=1}^{n} \frac{s_i}{\lambda_i} \tag{2}$$

Where R is the thermal resistance of the element [(m²K/W)], and s_i and λ_i are the thickness [m] and thermal conductivity [W/(mK)] of each i layer of the wall.

Also, ISO 9869-1 provides an experimental approach to determine the thermal resistance. Such standard establishes that the thermal resistance of an element can be obtained by the sum of the differences of internal ($T_{s,in,j}$) and external surface temperatures of the element ($T_{s,out,j}$) and the sum of heat fluxes (q_j):

$$R = \frac{\sum_{j=1}^{n} (T_{s,in,j} - T_{s,out,j})}{\sum_{j=1}^{n} q_j} \tag{3}$$

Both approaches have difficulties to be implemented in basement walls. Regarding the method from ISO 6946, knowing exactly the composition of the wall can be difficult so that the application of the method can be something of a challenge, and even little representative results can be obtained. As for the method from ISO 9869-1, the measurement of the external surface temperature has operational limitations because it would be necessary to undertake earthmoving works in order to place probes. For this reason, its practical application to this kind of walls would also be limited.

The feasibility of determining the thermal resistance of the wall was therefore analysed by measuring both the ground temperature and the external air temperature. Such tasks were performed with advanced regression models (see subsection 2.3 for further information).

2.2. Regression algorithms

Given that this methodological approach aims at determining the R of basement walls, various regression algorithms were used. Three different regression algorithms were used: multilayer perceptron, M5 Prime, and random forests. Such algorithms were selected because of their great performance in several research works, as can be seen in the following subsections.

2.2.1. Multilayer perceptron

The artificial neural networks are a computational paradigm tackling a huge variety of nonlinear statistical problems [68]. This algorithm imitates the hardware structure of the nervous system with the aim of building adaptive and parallel processing information systems which can estimate an efficient response. Several research studies are based on the potential of using multilayer perceptrons (MLPs) as architecture of artificial neural network [69], mainly due to their capacities of universal approximation [70]. The architecture of MLPs is made up of three or more layers (see Figure 2): an input layer, one or several intermediate layers, and an output layer. The output value of the neurons of each layer is obtained by the sum of the input values of the nodes of the previous layer, thus weighting the values with synaptic weights and using an activation function. The values of each neuron are spread to the last neuron of the output layer, which gives the estimated value of the MLP:

$$\hat{Y}_{MLP} = \sigma\left(\sum_{j=1}^{M} w_{kj}^{(2)} \sigma\left(\sum_{i=0}^{d} w_{ji}^{(1)} x_i\right) + w_{k0}^{(2)} y_0\right) \tag{4}$$

Where $\hat{Y}_{MLP}$ is the output value of the MLP, σ is the activation function, $w_{kj}^{(2)}$ are the weights of the output layer, $w_{ji}^{(1)}$ are the weights of the hidden layer, x_i are the values of the input layer, $w_{k0}^{(2)}$ and y_0 are the weight and the input value of the bias neuron of the hidden layer, respectively.

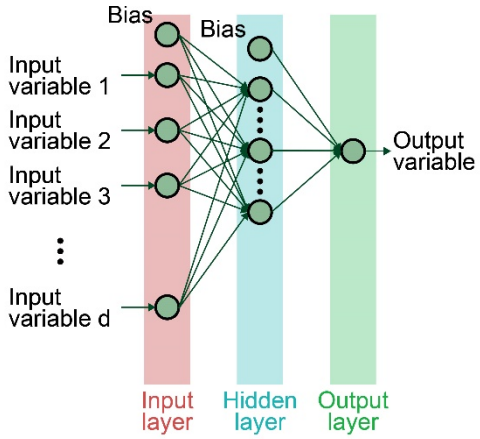

Figure 2. Scheme of an MLP model with one hidden layer.

Several studies on the characterization of thermal properties of elements are as follows: (i) Bienvenido-Huertas et al. [61] developed MLPs to carry out the post-processing to correct heat storage effects in thermal transmittance analyses. Adjusted estimations in the thermal transmittance value were obtained with respect to the reference values; (ii) Buratti et al. [71] generated an artificial neural network model to estimate the thermal transmittance of wooden windows. The results obtained estimations of the thermal transmittance value with an error lower than 1% with respect to the reference values; and (iii) Mitra et al. [72] developed MLPs to estimate the thermal resistance of handloom cotton fabrics. Adequate estimations were found, with a correlation coefficient between 86 and 90%.

2.2.2. M5 Prime

The M5 Prime (M5P) algorithm is an evolution of the classification and regression tree algorithm [73,74]. The classification and regression tree algorithm develops prediction models with a reverse tree structure (i.e., from the root to the leaves, with the root being in the upper part of the classification and regression tree model [75]). They are characterized by dividing the input space into subregions, thereby simplifying complex problems with simple models [76]. The reverse tree models are made up of internal nodes corresponding to the input variables, arches corresponding

to the values of the source node, and leaves corresponding to the value of the dependent variable. The structure of the model finishes in the leaves of the tree, which correspond to an output value of the model. Such scheme allows the models to be easily understood by users, a characteristic which other algorithms, such as MLPs, do not have [77].

Regarding the M5P algorithm, its main difference is the combination of the reverse tree structure with multivariant regressions (see Figure 3): the leaves of the model replace a unique output value with multiple linear regressions (MLRs) (see Eq. (5)). M5P generates therefore an MLR model for each subregion. When generating the model, M5P minimizes the internal variation of the subsets for the values of each branch. After developing the model, the overfitting of the model is generalized and reduced by applying the pruning (i.e., by removing the inefficient nodes) [78]. Hence, the main advantages of the M5P models are their robustness when there is a lack of values in some data, as well as the possibility of using many numeric variables efficiently [79,80].

$$MLR = \beta_0 + \sum_{i=1}^{v} (\beta_i v_i) + \varepsilon \quad (5)$$

Where β_0 is the independent term, β_i are the regression coefficients, v_i are the independent variables, and ε is the error.

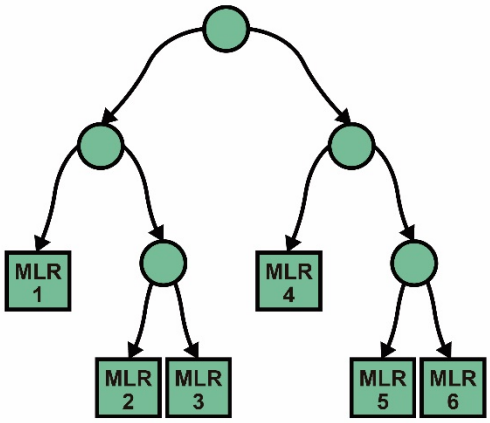

Figure 3. Scheme of an M5P model.

As a result, the M5P algorithm is more and more used in the field of energy analysis, both in market and buildings: (i) Azofra et al. [81] analysed the influence of thermal solar energy, biomass, and hydraulic power on the electricity price. To estimate the energy price without using such renewable sources, an M5P model was developed. The correlation obtained by the model was 85%. In later studies, the authors analysed the influence of other renewable energies variables, such as wind power [82] or photovoltaic technology [83], on energy prices by using M5P; (ii) Pallonetto et al. [84] evaluated the use of control algorithms to implement response strategies in the energy demand of residential buildings. Regression algorithms were used to determine the temperature differential. For this purpose, the use of M5P was compared with the use of MLP. More accurate estimations were obtained for M5P, with an increase of the correlation coefficient greater than 10% in the different models analysed; and (iii) Afsarian et al. [85] used an M5P model to estimate the total energy consumption in a reference building. The results obtained correlation coefficients greater than 90% in most data.

2.2.3. Random forests

The advantage of the classification and regression tree algorithm is that the structures of the model generated are easy to understand. However, several studies have discussed the limitations of such model to carry out adequate estimations in new instances [86,87]. For this reason, the random forest (RF) algorithm is a modification of the model. The characteristic of RF is that, instead of generating a unique tree model (as the classification and regression tree algorithm), a forest of tree models is created (see Figure 4), thereby reducing the error and the variance of the model [88,89]. Like M5P, RF uses great datasets and is robust when there are atypical values [90]. For the training of the model, the algorithm takes N bootstrapped sample sets from the dataset [89] (bootstrap is a method to estimate the sampling distribution of an estimator by sampling with replacement from the original sample [91]). Each bootstrapped sample develops a tree model, and each node of the model is divided by using a subset of m predictors randomly selected, thus reducing the effect generated by the strongest predictors [78]. The output value of the model is obtained through the average value of the estimations carried out by the various tree models of the forest (see Eq. (6)). So, RF fits many classification and regression tree models to a dataset and then combines the predictions from all the trees. The difference between M5P and RF is that the former obtains the output value through the MLR in the leaf, while the latter obtains it through the value of each leaf.

$$\hat{Y}_{RF} = \frac{1}{T}\sum_{t=1}^{T} \hat{Y}_t \quad (6)$$

Where T is the number of tree models, and $\hat{Y}_t$ is the output of the t-th tree.

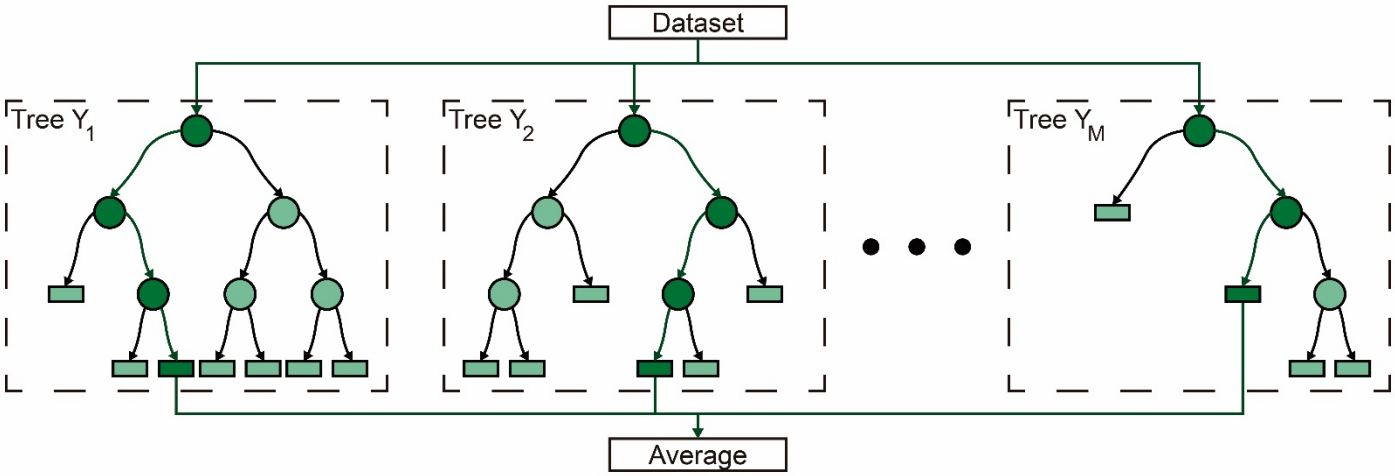

Figure 4. Scheme of an RF model. For the reader's understanding of how the model works, the response values of each tree of the forest are represented in a darker colour.

Such model is widely used in the field of building analysis and evaluation: (i) Cui et al. [92] developed RF models to estimate the average internal temperature difference in spaces connecting two areas (e.g., open stairwells between two floors). The error in the estimations of the RF models was lower than other regression algorithms, such as artificial neural networks or the support vector regression; (ii) Kontokosta and Tull [93] used three different regression models to estimate the city-scale energy use in buildings: RF, MLR, and support vector regression. Acceptable estimations were obtained with the three algorithms; and (iii) Ghahramani et al. [94] used various algorithms of classification to predict the occupants' interactions from the ambient sensing technologies. Random forests obtained better predictions than other algorithms, such as the decision tree or the support vector machine.

2.2.4. Training and validation of the regression models

To estimate the thermal resistance of the basement walls, input values corresponding to averages of five variables easily measurable were used (see Table 1). The average value is obtained by adding the values of each variable and dividing it by the number of instances. Variables related to the external surface of the wall (e.g., external surface temperature) were not used. As the adequate time window was unknown (i.e., how much time should last the monitorings), 4 time windows were established: (i) 0.5 day; (ii) 1 day; (iii) 1.5 days; and (iv) 2 days. Various datasets were generated for each time window, and different models were therefore developed according to the training data used. The use of various time windows determined the most acceptable duration to monitor the element due to their influence on input variables.

Table 1. Input and output variables of the regression models.

Input variables	Output variables
$\overline{T}_{external}$, $\overline{T}_{ground}$, $\overline{T}_{surface-internal}$, $\overline{T}_{internal}$, $\overline{q}$	$R_{w;b}$

$\overline{T}_{external}$: average of the external air temperature [ºC]; $\overline{T}_{ground}$: average of the ground temperature [ºC]; $\overline{T}_{surface-internal}$: average of the internal surface temperature of the basement wall [ºC]; $\overline{T}_{internal}$: average of the internal air temperature [ºC], and $\overline{q}$: average of the heat flux [W/m²].

The creation of the training and validation datasets is explained below. The dataset containing the data of the hot-box test was made up of 480 instances, and the dataset of simulated data of basement walls of 10,579 instances. Despite using different time windows, the number of observations of the training samples was identical for each test. Also, the instances used in each training dataset were the same (i.e., in a measurement, one of the records is used to calculate R and the average values in the four time windows).

The dataset of each test was generated, and then divided into two subsets: (i) the training subset corresponded to a random sampling of 75% of instances of the dataset, and (ii) the testing subset corresponded to the remaining 25%. The training subsets were used to generate individual models for each time window and regression algorithm, so 12 various regression models were created in each test (i.e., 4 different model for each regression algorithm). For the training of the regression models, a 10-fold cross validation was carried out, thus reducing the variance of the models [95]. All training subsets were randomly divided into 10 folds: 9 folds were used for the training, and the remaining fold for the testing. This process was performed 10 times. The performance of each model is obtained by the mean value of the 10 folds. The testing dataset was used to evaluate the performance in instances which were not used in the training. The performance of the regression models was analysed by evaluating three statistical parameters: the mean absolute

error (MAE) (see Eq. (7)), the root mean square error ($RMSE$) (see Eq. (8)), and the coefficient of determination (R^2) (see Eq. (9)).

$$MAE = \frac{\sum_{i=1}^{n} |t_i - m_i|}{n} \tag{7}$$

$$RMSE = \left(\frac{\sum_{i=1}^{n} (t_i - m_i)^2}{n} \right)^{1/2} \tag{8}$$

$$R^2 = \frac{\sum_{i=1}^{n} \frac{(m_i - \overline{m}) \cdot (t_i - \overline{t})}{n-1}}{\sqrt{\sum_{i=1}^{n} \frac{(m_i - \overline{m})^2}{n-1} \cdot \sum_{i=1}^{n} \frac{(t_i - \overline{t})^2}{n-1}}} \tag{9}$$

Where m_i is the estimated value, t_i is the actual value, and n is the number of instances in the dataset.

Regarding the configuration of the regression algorithms, some aspects are as follows: (i) for the MLP models, architectures of 3 layers were used (i.e., with one hidden layer). A sigmoidal function was used as a transfer function (see Eq. (10)). The MLPs were trained by backpropagation [96] and the Broyden-Fletcher-Goldfarb-Shanno algorithm [97] was used. A learning rate of 0.3 and a momentum of 0.2 were used as fixed parameters. The number of neurons of the hidden layer was varying until determining the most appropriate architecture (the number of neurons in the hidden layer analysed oscillated between 3 and 12); (ii) the M5P models were generated by using the pruning to reduce the variance of the models; and (iii) the RF models were created by varying the number of trees until determining the most acceptable configuration (the number of trees analysed oscillated between 1 and 150).

$$f(x) = \frac{1}{1 + e^{-x}} \tag{10}$$

2.3. Hot-box test

As indicated above, the methodology was first analysed under controlled conditions in laboratory. The installation was a calibrated hot-box (CHB) designed according to ISO 8990 [98]. The walls of the CHB were made up of three layers: a first layer of two polypropylene sheets of 3 mm, which were separated by an internal air gap of 2 cm; a second layer of 8 cm of polyurethane (with a thermal conductivity of 0.023 W/(mK)); and a third layer of oriented strand board of 1 cm, with a thermal conductivity of 0.13 W/(mK). The CHB was heated by electrical resistance, whereas it was cooled by a cooling thermoelectric system equipped with ventilators. The air conditioning systems of the CHB were controlled by programmable thermostats and voltage regulators which maintained the programmed setpoint temperatures in the interior of both spaces.

The peculiarity of this CHB is that the cold chamber was filled up with soil (see Figure 5 and Figure 6). All the volume directly in contact with the sample was filled in and compressed, and the remaining volume was used for the cooling of the cold chamber. The sample used was a mass concrete wall of 6 cm of thickness. The height of the sample did not reach the whole the internal height of the box, and the remaining space was covered with an insulating panel of extruded polystyrene of 10 cm of thickness. The objective was to have all the space of the sample in contact with the ground when the box is filled up with soil, but there was a low volume simulating the conditions of the external temperature.

A total of 6 tests were performed, varying both the depth at which the temperature probe of the ground was placed (20 and 30 cm) and the thermal gradient between both chambers (30, 40, and 50 ºC). These thermal gradients were selected due to the recommendations of some studies to reach high values [99]. Each test lasted 8 days and the interval of data acquisition was 10 min. To perform the tests, 3 data loggers with probes were used to measure the ground temperature, the surface temperatures, the air temperature, the air relative moisture, and the heat flux of the sample. Table 2 indicates the equipment used and their technical characteristics. Also, an infrared camera (FLIR E60bx) was used to analyse the temperature distributions throughout the test.

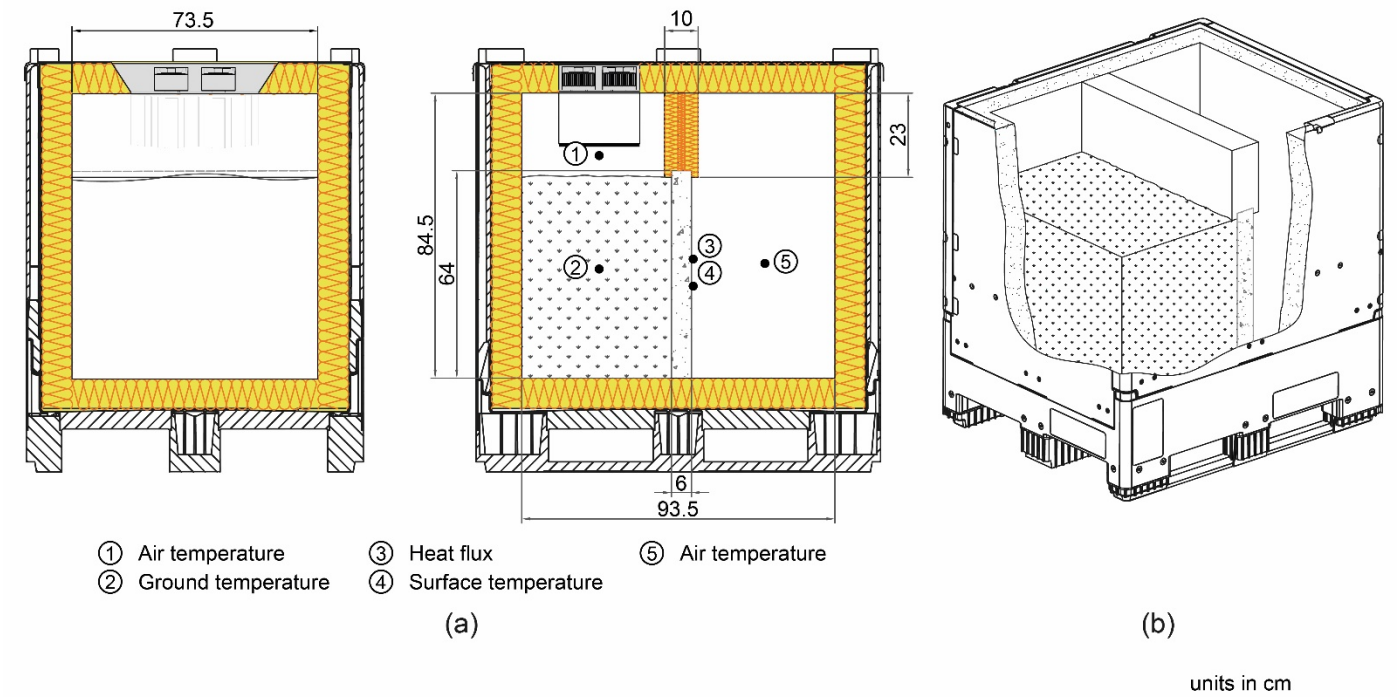

Figure 5. CHB in the approach in which soil is used: (a) sections of the CHB, and (b) perspective of the CHB.

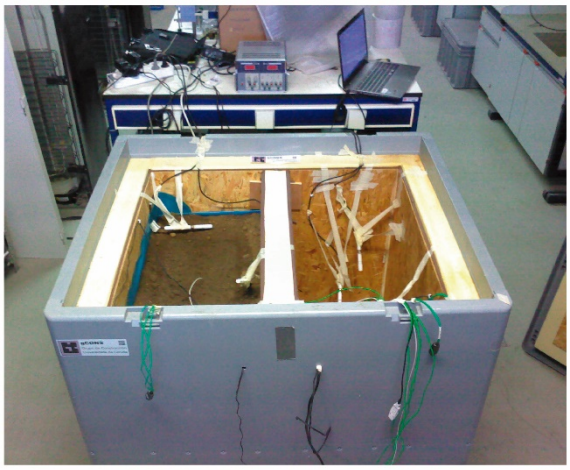

Figure 6. External photograph of the CHB in the approach in which soil is used.

Table 2. Main technical specifications of the equipment.

Equipment	Input	Measuring range	Accuracy
Data logger ALMEMO 2590-4AS			
with temperature sensor Pt100	Temperature	-30 to 150 ºC	±0.15 K +0.002%
with thermocouples T 190-2	Temperature	-10 to 105 °C	±0.05 K ±0.05%
with the heat flux plate FQA018C	Heat flow	-40 to 80 ºC	±5%
Data logger TESTO 435-2			
with thermocouples 0614 1635	Temperature	-20 to 70 ºC	±0.1 ºC
Data logger CAMPBELL CR1000			
with temperature probe	Temperature	-50 to 100 ºC	±0.1°C
Infrared camera FLIR E60bx	FOV	25°x19°	
	IFOV	1.36 mrad	
	Sensor	FPA, uncooled microbolometer	
	Spectral range	7.5-13 µm	
	Thermal sensitivity	<0.05-30 °C	

The data obtained from the monitoring of the sample were used to develop various regression models. Data were grouped in a unique dataset from which average values and results of thermal resistance were used by using the four time windows (see Section 2.2.4). Such data were used to generate regression models with the 3 algorithms of this study. With this first phase, the possibility of using the methodology under controlled conditions could be previously evaluated to analyse later its use in actual tests.

2.4. Tests in buildings

After analysing the possibility of using the methodology under controlled conditions in laboratory, it was implemented in two actual case studies. Both case studies had inhabitable rooms in contact with the ground. In addition, they were selected because the basement walls were distinctly designed and representative of the building stock. One of the case studies constituted a reinforced concrete wall without other layers, whereas the other case study was made up of a composition of layers, including insulating material. This aspect could be determined because the layers of the basement walls were accurately known (see Figure 7), thereby characterizing the thermal resistance of the walls according to the methodology of ISO 6946 (see Eq. (2)). Both case studies had an inhabitable room, where the internal probes were placed, at a depth of less than 3 m because of two reasons: (i) it is one of the most common dwelling typologies in contact with the ground, and (ii) it simplifies the research. Future research studies could be focused on the feasibility of analysing case studies more deeply.

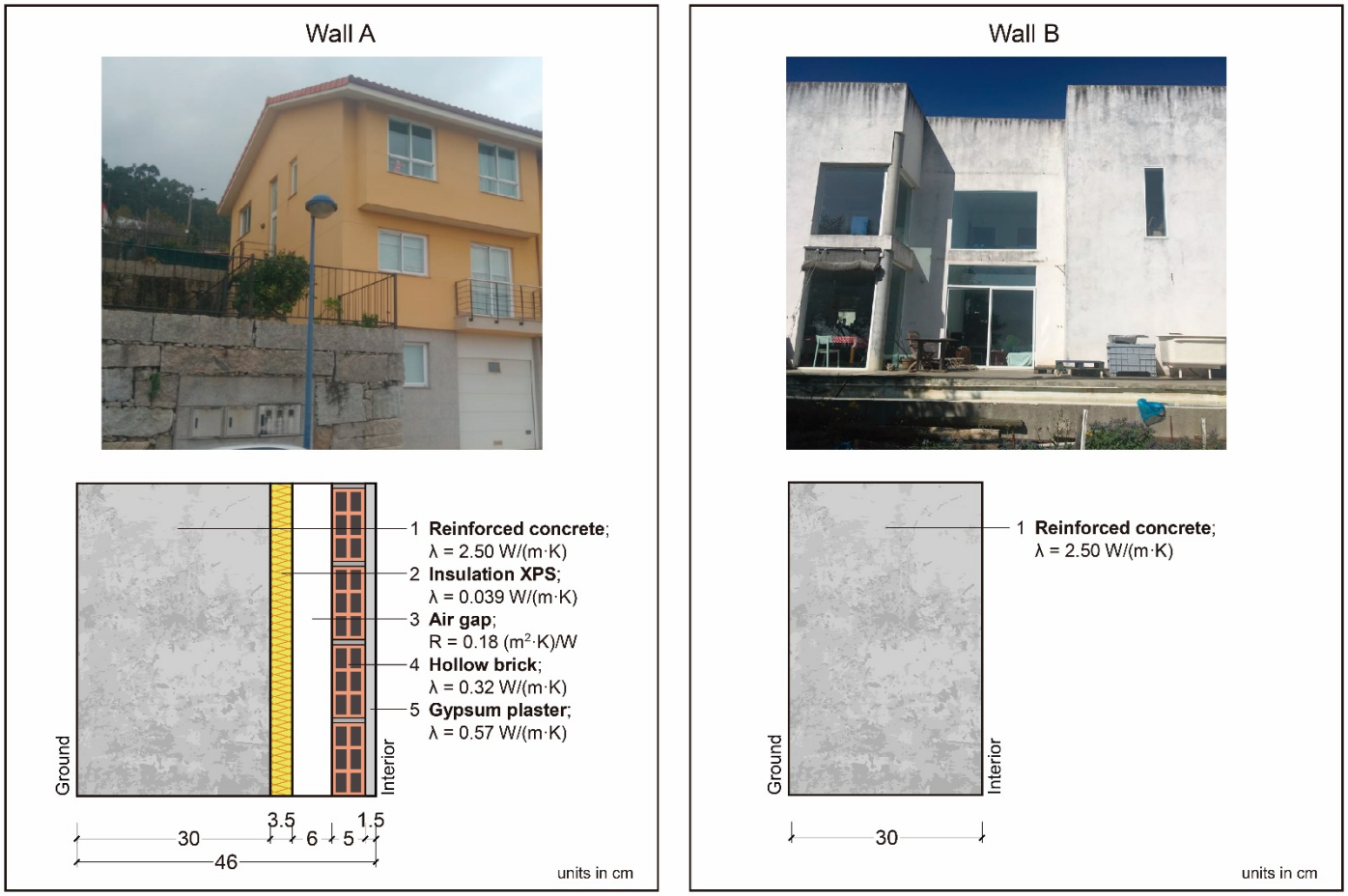

Figure 7. Thickness and thermophysical properties of the actual basement walls analysed.

Tests lasted 2 days, and the interval of data acquisition was 10 min. Monitorings were performed by using the same equipment as in the test of the CHB (see Table 2). The criteria of placing were as follows (see Figure 8): (i) the temperature probe of the ground was placed at 50 cm from the limit of the wall, and at a depth of 50 cm. A greater depth was not used because of the possible limitations for placing the probe when performing tests (e.g., resistance of the ground or damages in the external areas of the building). Also, the use of such distance guarantees that the variation of the humidity content in the ground is negligible because variations are not presented until reaching 2 m [100]; (ii) the probe of the external air temperature was placed 30 cm from the façade and at a height of 1 m; (iii) the heat flux plates and the surface temperature probes were placed at a height of 1 m above the level of the ground and separated from corners and wall joints; and (iv) the probes of internal air temperature were placed at a height of 1.5 m above the floor of the room.

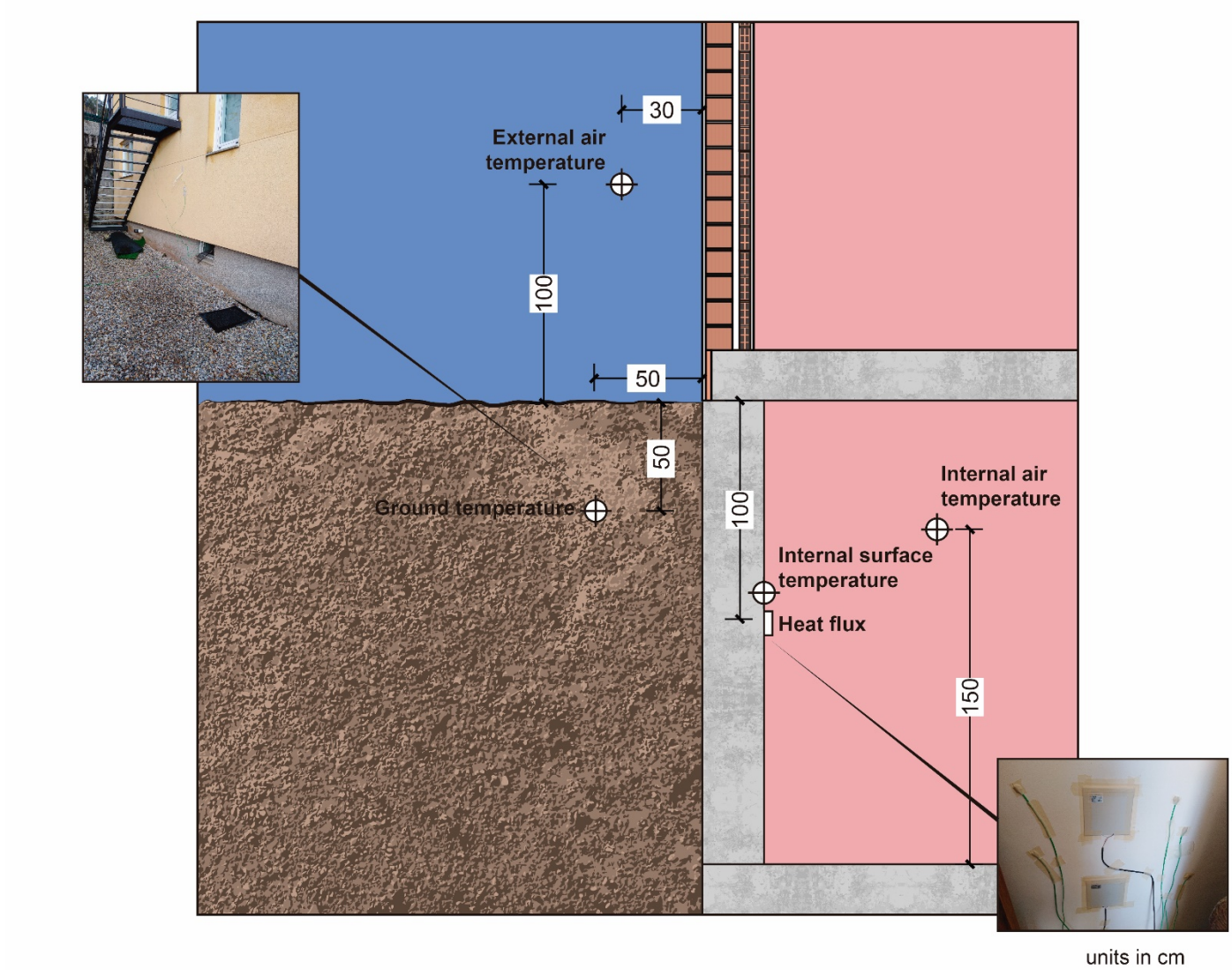

Figure 8. Methodology of placing the equipment in the actual case studies monitored.

2.5. Two-dimensional simulations of the thermal resistance for the dataset of actual case studies

Despite the monitorings in the 2 actual case studies, the regression models for actual case studies could not be generated by using the data obtained due to the need for creating models able to be adapted to any test performed in basement walls. Two-dimensional simulations were therefore performed by means of FEM to generate robust datasets to train the regression models and estimate the thermal resistance of actual case studies. Each simulation was included in the dataset of actual cases as an observation. So, simulations were first used to train and assess the regression models developed for actual cases, and then to estimate $R_{w;b}$ in both walls (see section 2.4). Simulations were made with the HTflux software, and a total of 149 time series of monitorings carried out in previous research works were introduced [37,101]. The simulation models were designed following the criteria set up in the ISO 10211 [102]. A total of 71 various typologies of basement walls were configured, and 10,579 simulations were obtained by combining time series. Basement walls representing building typologies in Spain were modelled. Several sources from various studies were used [103,104], as well as the technical standard in Spain [105]. The aim was to use the methodology in various typologies of basement walls. For each simulation, the thermal resistance, the average temperature and heat flux values were obtained by using the time windows indicated above. The temperature and heat flux were measured by following the same scheme in Figure 8. Due to the variability of the heat flux through the wall because of the two-dimensionality acquired by the effect of the ground, the simulations were also performed considering the one-dimensionality of the wall (see Figure 9). Thus, the thermal resistance values were calculated without the two-dimensional effect of the ground for three reasons: (i) to be able to identify precisely whether the knowledge of the wall is real (i.e., whether both layers and their characteristics are real); (ii) to be used in the analysis of the thermal performance of the basement wall, as included in ISO 13370 [57]; and (iii) to carry out energy analysis of the building by using simulation softwares, such as DesignBuilder. The proposed methodology could also be used to obtain two-dimensional thermal resistances, although its potential of use is reduced due to the aspects mentioned above. In addition, representative comparisons of the value obtained with the reference value of ISO 6946 cannot be made. In this way, the criterion of ISO 9869-1 was used to consider whether the estimations carried out by the regression models ($R_{\text{Estimated}}$) were representative: those

estimations with a deviation lower than 20% with respect to the reference value ($R_{\text{Reference}}$) can be considered representative (see Eq. (11)).

$$\text{Deviation} = \frac{R_{\text{Estimated}} - R_{\text{Reference}}}{R_{\text{Reference}}} \tag{11}$$

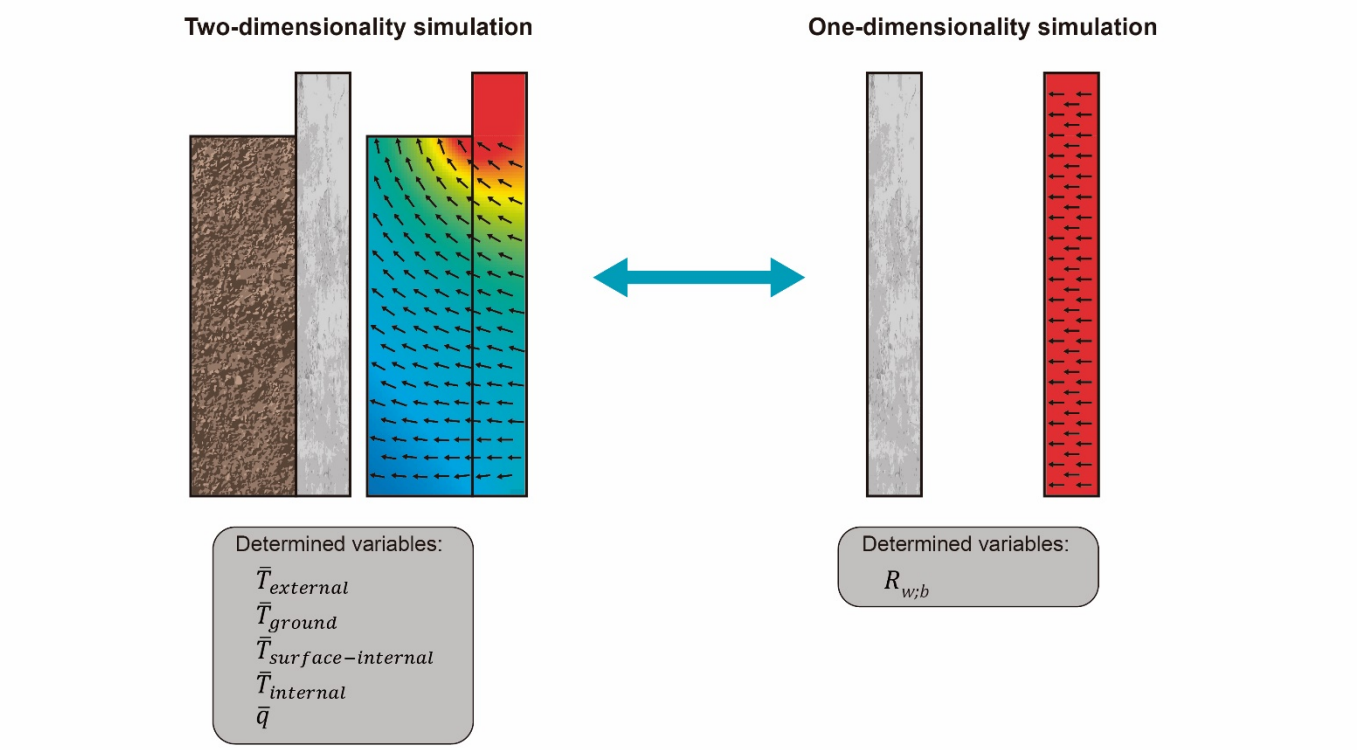

Figure 9. Scheme of the relation between the two-dimensional and one-dimensional analysis used to generate the simulations.

3. Results and discussion

3.1. Calibrated hot-box test

As mentioned in Section 2, an analysis was first carried out in a CHB which was adapted to assess the possibility of using the proposed methodology under controlled conditions in laboratory before analysing it in actual case studies. Given such analysis using the CHB aims at simulating the performance of the sample similarly as under actual conditions, two aspects should be stressed concerning the ground: (i) an isotherm profile along the section of ground, and (ii) the temperature value of the ground should be constant due to the temperature values of the cold and hot chambers.

The fulfilment of such conditions was therefore one of the first aspects analysed. Firstly, thermographies taken in sections of the ground and located in the cold chamber allowed different isotherms to be visualized (see Figure 10 (a)). The temperature values in the lower part of the ground were greater than in the upper part (in contact with the air of the cold chamber), thereby simulating the real behaviour of a basement wall in cold seasons, when the ground temperature was higher in levels of greater depth (see Figure 10 (b)). Secondly, the analysis of the temperatures recorded in tests allowed the stability of the ground temperature value to be verified. As can be seen in Figure 11, the time required to stabilize the temperature value of the ground was 60 hours. The test with a depth of 30 cm was performed after the test with a depth of 20 cm, thus implying that the ground temperature was steady since the beginning of the test. Such analysis was also useful to corroborate the existing isotherms in the ground because the ground temperature had an average value of 22.4 ºC for the depth of 20 cm, whereas the average value of the ground temperature was greater for the depth of 30 cm.

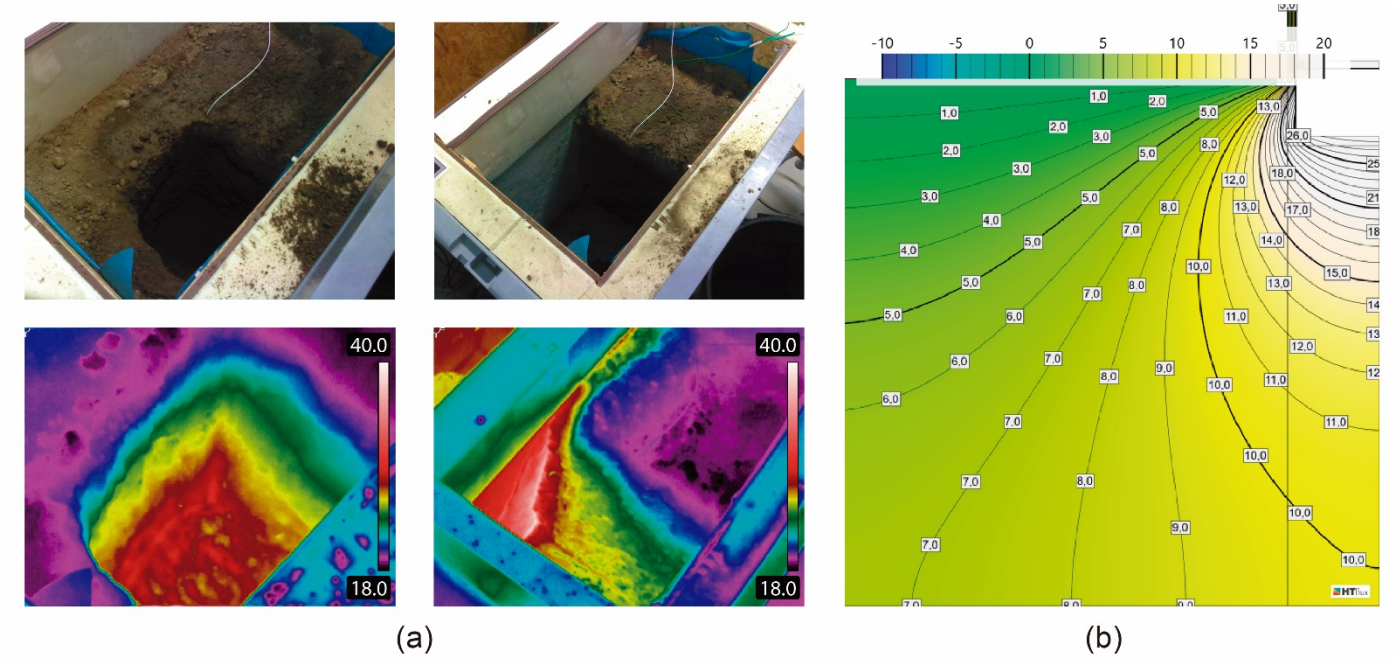

Figure 10. Analysis of the distribution of isotherms in the CHB: (a) thermographies of the ground temperature profile of the CHB, and (b) example of the distributions of isotherms in an actual case study.

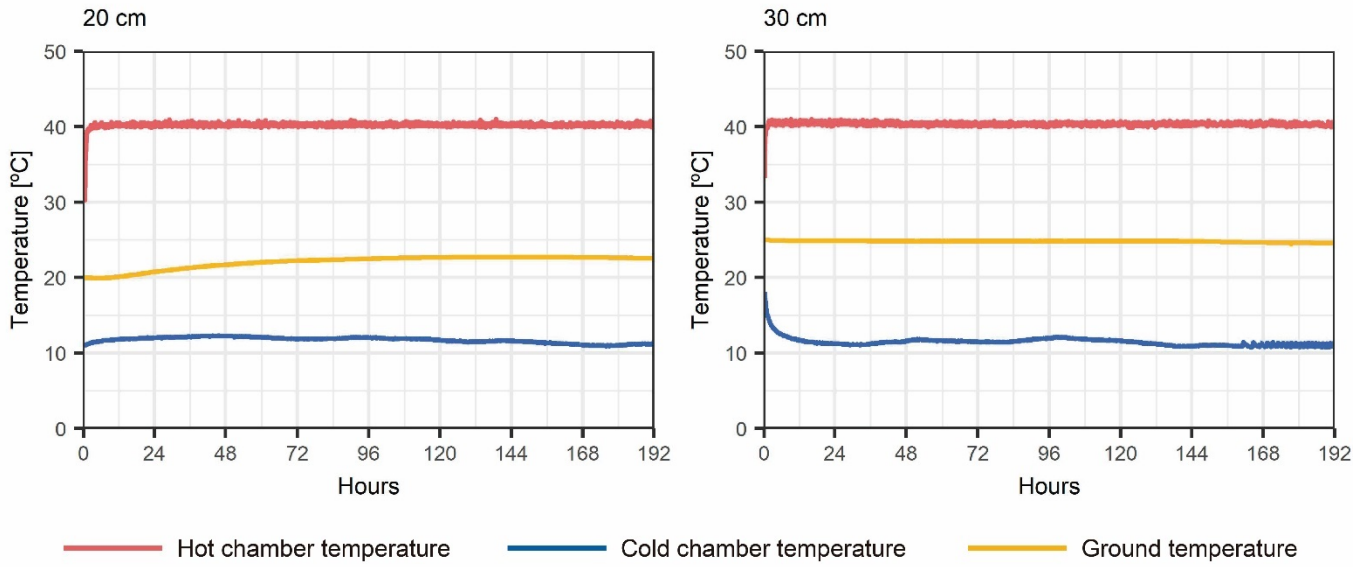

Figure 11. Variation of the ground temperature in the tests performed in the box. Example of tests with a temperature differential of 40 ºC.

After analysing how the CHB represents the behaviour of a basement wall in a controlled environment, the performance of the regression models was analysed. As indicated in Section 2, monitoring data were used to generate the training and testing subsets, as well as the four time windows considered in this study (0.5 day, 1 day, 1.5 days, and 2 days). Table 3 represents the performance results from the training and testing. Figure 12 shows the point clouds between the actual and the values estimated by the regression models. It is worth stressed that the difference in the values shown by the point clouds is due to the variation presented by $R_{w;b}$ because it was obtained through different time windows. The performance obtained by the models were quite adjusted. Both in training and testing, the determination coefficient had values greater than 99% in all models. Likewise, MAE and $RMSE$ were almost in all models lower than 0.0005 and 0.00010, respectively, and only in some models the error parameters were higher than such values, although the increase of the error parameters was very low (0.0003 or lower). The regression algorithms had also very similar performances. The estimations carried out by M5P, MLP, and RF were very similar, thereby presenting point clouds with estimated values close to the actual values. On the other hand, the time window with the best performance in the estimations of the models could not be determined. For all time windows, the performance in the testing obtained R^2 greater than 99.90% with error parameters. It was only found that the use of time windows higher than 0.5 day allowed a slight decrease in the error of the estimations to be achieved. The analysis using the CHB could therefore determine the effectiveness of using regression algorithms to make accurate estimations of $R_{w;b}$. Then, the use of the methodology in actual case studies was analysed. Also, the design of CHB for samples in contact with the

ground is appropriate to simulate the two-dimensional behaviour under controlled conditions in laboratory. Such design is an opportunity to reproduce and analyse various building solutions and their thermal performance.

Table 3. Behaviour in training and testing phases of regression models in the CHB test.

Model	Training			Testing		
	R^2 [%]	MAE	$RMSE$	R^2 [%]	MAE	$RMSE$
Time window of 0.5 day						
M5P	99.91	0.0005	0.0009	99.92	0.0005	0.0009
MLP	99.96	0.0005	0.0006	99.98	0.0004	0.0005
RF	99.97	0.0003	0.0005	99.98	0.0003	0.0005
Time window of 1 day						
M5P	99.84	0.0007	0.0013	99.92	0.0005	0.0009
MLP	99.98	0.0004	0.0005	99.99	0.0002	0.0003
RF	99.98	0.0003	0.0004	99.99	0.0003	0.0004
Time window of 1.5 days						
M5P	99.89	0.0007	0.0010	99.89	0.0007	0.0010
MLP	99.98	0.0003	0.0005	99.99	0.0002	0.0003
RF	99.95	0.0003	0.0007	99.97	0.0003	0.0005
Time window of 2 days						
M5P	99.91	0.0006	0.0010	99.92	0.0005	0.0009
MLP	99.97	0.0004	0.0005	99.98	0.0003	0.0004
RF	99.98	0.0003	0.0004	99.99	0.0003	0.0003

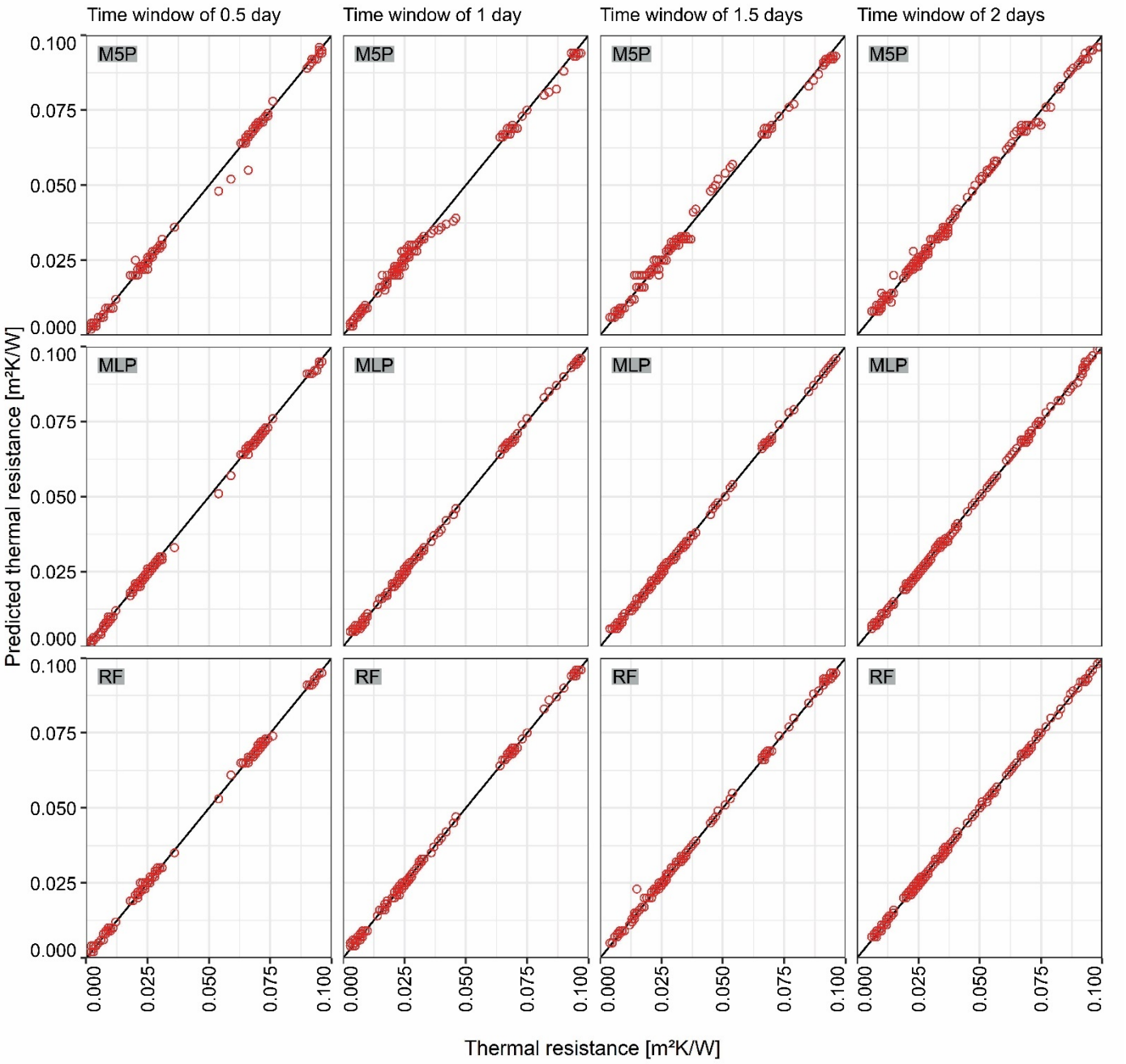

Figure 12. Point clouds between the actual and predicted thermal resistance values. Results of the data obtained in the CHB test.

3.2. Test in actual case studies

Firstly, the dataset used to train the models was created in this second phase. As mentioned in Section 2, two-dimensional simulations were carried out by using FEM of 71 various typologies of basement walls, thereby obtaining a total of 10,579 simulations. Unlike in the test with the CHB (in which there was only one kind of case study), in this case the performance obtained by the models was supposed to be different from that obtained in the previous phase because of high number of various walls. Table 4 indicates the values of the statistical parameters obtained in the training and testing of the models. Figure 13 shows the adjustment degree of the estimated values for each instance of the testing subset. Unlike in the regression models with data of the CHB, the performance of the models in this case had two tendencies. On the one hand, the tree models (M5P and RF) had very adjusted performances in the time windows, whereas MLP had the worst performance. Also, R^2 had values between 98.81 and 99.86% in the tree models, whereas it oscillated between 90.09 and 97.03% in MLP. The best correlation coefficient obtained by MLP (in the testing of the time window of 2 days) was therefore 1.78% lower that the worst R^2 obtained by the tree models (the value obtained in the training of M5P of the time window of 0.5 days). However, the worst performance of MLP was found in the error parameters. Both in the training and testing, MAE and RMSE had increases with respect to the parameters of the tree models greater than 254.55% and 155.56%, respectively. The adjustment degree of the MLPs was therefore very low with respect to the simulated data. Regarding the comparison between M5P and RF models, the performance of such models were similar, although RF obtained a better degree of adjustment. RF had R^2 with increases greater than 0.22%

with respect to M5P, and values of MAE and RMSE with decreases greater than 0.017 and 0.018, respectively. Therefore, the use of a greater number of walls in the dataset generated a lower adjustment in the MLP estimations compared to the results of the CHB test.

Concerning the time windows used, it was found that as the time assigned to the window increased, the performance of the tree models improved, particularly in the statistical parameters of the testing. By increasing the window in 0.5 days, R^2 improved more than 0.16 and 0.06% in M5P and in RF, respectively. Also, the values of the error parameters decreased as the time window increased: (i) for M5P, MAE and RMSE presented decreases greater than 0.008 and 0.004, respectively; and (ii) for RF, MAE and RMSE had decreases greater than 0.003 and 0.007, respectively. Error parameters slightly worsened only in the time window of 1.5 days, although the increase of a window of 2 days achieved the best estimations.

Table 4. Behaviour in training and testing phases of regression models in FEM simulated data.

Model	Training			Testing		
	R^2 [%]	MAE	$RMSE$	R^2 [%]	MAE	$RMSE$
Time window of 0.5 day						
M5P	98.81	0.045	0.078	98.88	0.044	0.076
MLP	90.09	0.185	0.229	93.07	0.156	0.205
RF	99.51	0.020	0.050	99.50	0.021	0.050
Time window of 1 day						
M5P	99.26	0.035	0.064	99.04	0.036	0.072
MLP	91.42	0.174	0.219	95.43	0.150	0.184
RF	99.71	0.015	0.040	99.66	0.016	0.043
Time window of 1.5 days						
M5P	99.24	0.038	0.068	99.20	0.038	0.070
MLP	94.17	0.154	0.193	95.59	0.190	0.233
RF	99.73	0.016	0.041	99.72	0.016	0.042
Time window of 2 days						
M5P	99.59	0.031	0.054	99.63	0.030	0.051
MLP	96.10	0.137	0.171	97.03	0.243	0.281
RF	99.86	0.013	0.031	99.85	0.013	0.033

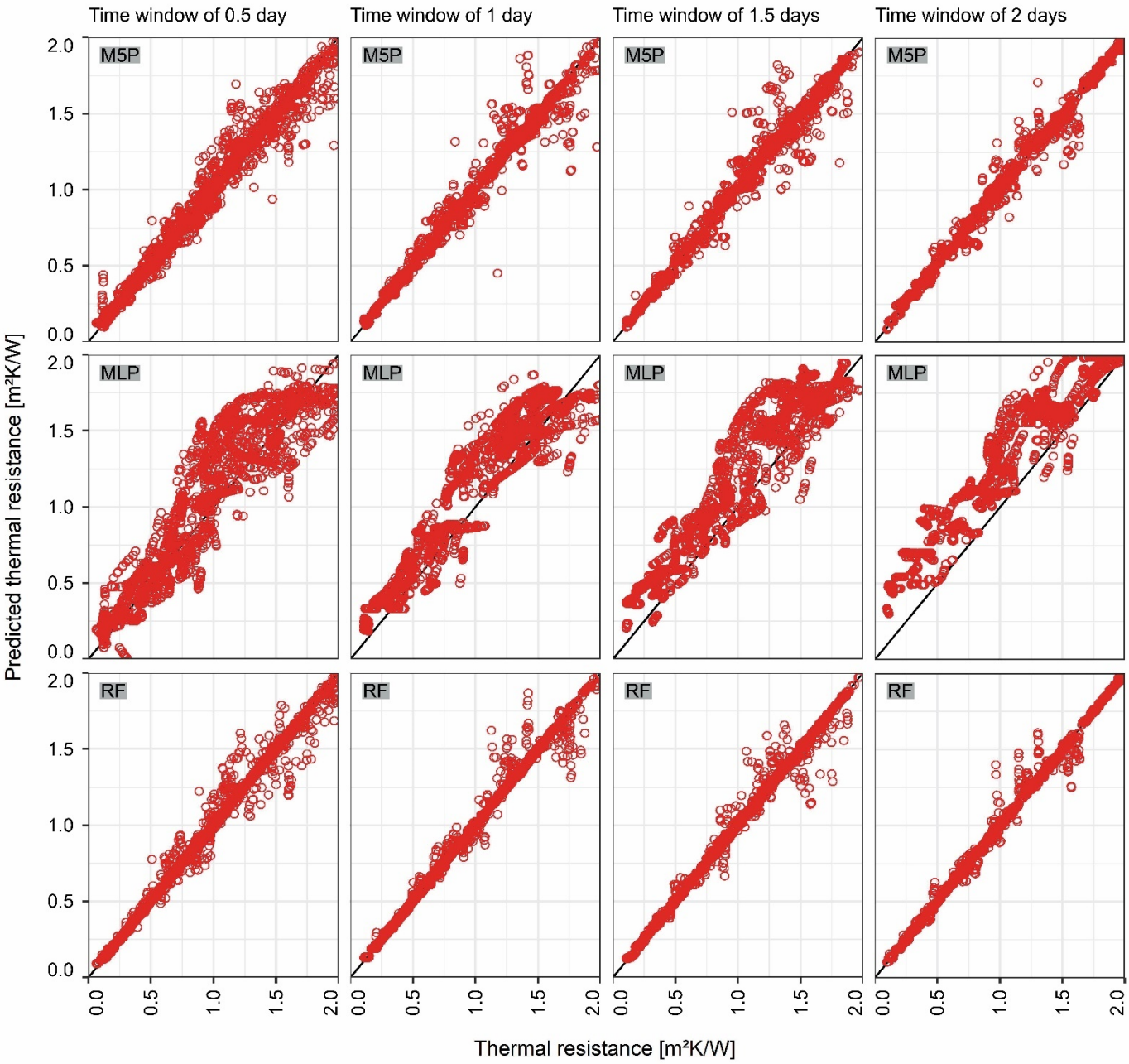

Figure 13. Point clouds between the actual and predicted thermal resistance values. Results of the data obtained in simulations of actual case studies.

Thus, the use of time windows of 2 days ensured an acceptable performance of the models, so it is the most appropriate time window for the method. Furthermore, the duration of the monitorings would be similar with other existing methods characterizing the envelope elements, such façades with ISO 9869-1. The performance of the estimations carried out by the method for both actual case studies was therefore made with the models of 2 days.

In relation to this aspect, actual basement walls were monitored in periods of 2 days (see Figure 14). By using the monitoring data, two input vectors (one by each wall analysed) could be generated for the regression models (i.e., the values of $\overline{T}_{external}$, $\overline{T}_{ground}$, $\overline{T}_{surface-internal}$, $\overline{T}_{internal}$, $\overline{q}$ in a time windows of 2 days for each wall were introduced in the regression models). Figure 15 represents the values of estimated thermal resistance by the regression models. For Wall A, M5P was the only model which achieved an estimation of thermal resistance with a deviation lower than 20% with respect to the reference value (2.90%), whereas MLP and RF had deviations of 65.94 and 51.45%, respectively. For Wall B, M5P was again the model estimating the most adjusted value of thermal resistance with respect to the reference value (with a percentage deviation of 12.50%), although RF made an estimation of thermal resistance which can be considered valid (although the percentage deviation was 20.83%, the absolute difference between both values was 0.135 m²K/W). Also, MLP was again the model which made the worst estimation. In this sense, estimations for MLP for both walls were quite similar: 0.47 m²K/W for Wall A, and 0.487 m²K/W for Wall B. This reflects the small capacity of generalization of MLP in new instances as well as its low performance with the configuration of the input variables considered. Consequently, the tree models have a capacity of generalization in new cases greater than MLP, with M5P being the best regression model to estimate more adjusted values. M5P constitutes therefore the most efficient option to process the data obtained in the monitorings of actual basement walls.

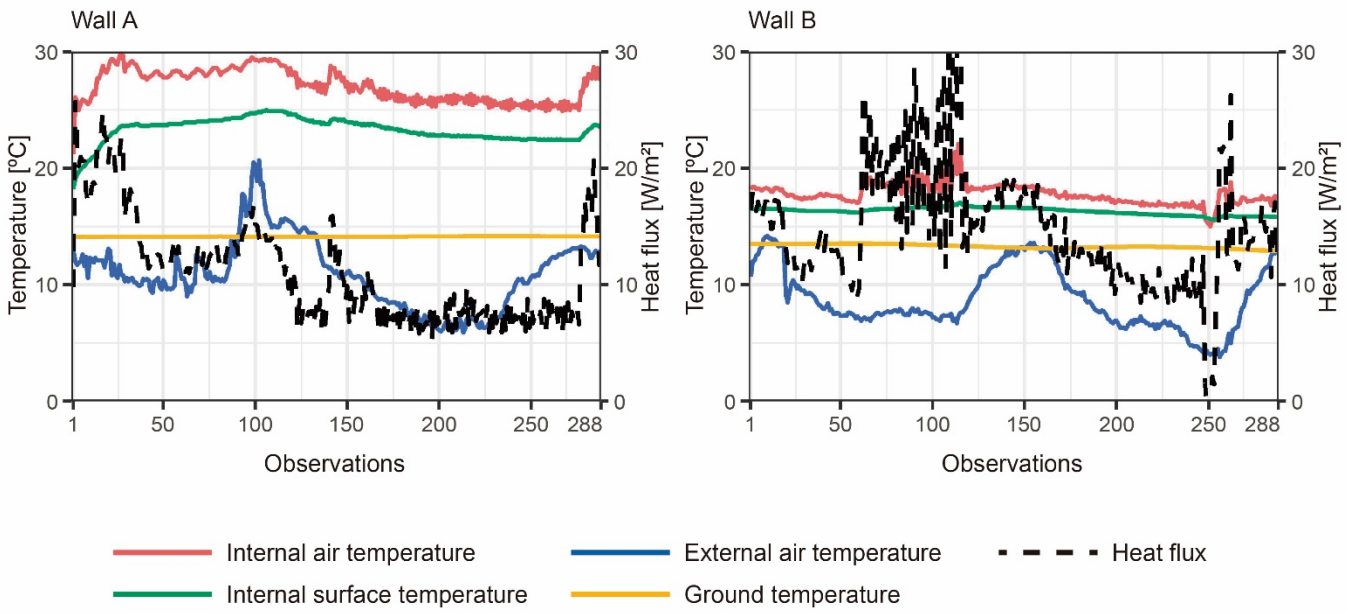

Figure 14. Time series of the variables measured in the actual case studies.

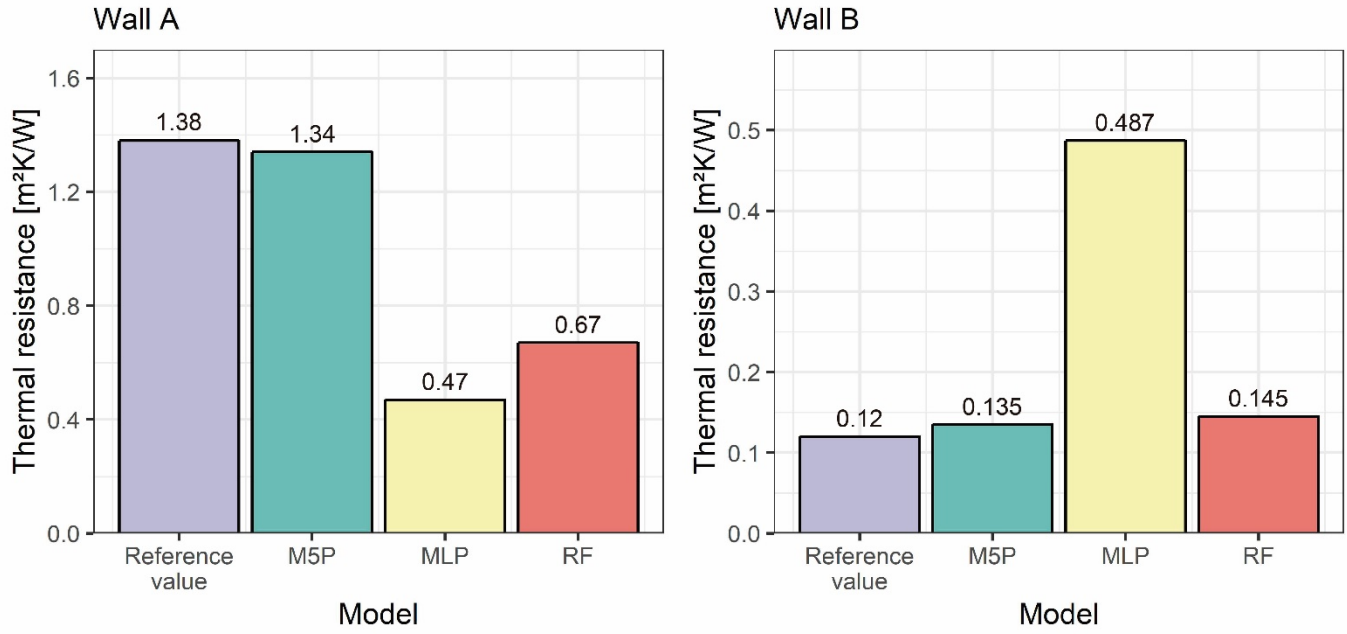

Figure 15. Comparison between the reference and estimated values of $R_{w;b}$ obtained by the regression models in both actual basement walls.

3.3. Potential and limitations of the methodology in actual walls

This methodology aims at characterizing the thermal resistance of basement walls (see Figure 16) and uses 5 average values as input variables $[\overline{T}_{external}, \overline{T}_{ground}, \overline{T}_{surface-internal}, \overline{T}_{internal}, \overline{q}]$ which are obtained by monitoring each wall for 2 days. Such variables are easily measurable by using temperature probes and heat flux plates, and the requirements for placing the probes which measure it have been previously explained in the subsection 2.4. The input vector is generated and introduced in the M5P model, thus obtaining the thermal resistance value of the model. The M5P model is developed with a dataset obtained through simulations as section 2.5 indicates. Simulations generate dataset without a huge temporary effort, thus implying a greater use of this methodology in actual problems.

The analyses methodology precisely determined the thermal resistance of the actual basement walls without presenting any decreases in the estimations made by the constructive composition of the walls. Also, both walls had characteristics clearly different, one of them having insulation and air gap, and the other being only a reinforced concrete layer. So, the M5P model was that with greater capacity of generalization. Given that the typologies of basement walls from various countries usually have similar characteristics, the possibilities of using the methodology are not only limited to the area where these case studies are located, thereby making evident its international importance. However, the analysis of the influence of various ground typologies should be evaluated, thereby implying the generation of different

models according to the existing ground. In addition, there may be limitations in measuring the ground temperature in those buildings where measurement is not possible (e.g., hidden ground by sidewalks). Likewise, variations in the heat flux of the wall or the temperature of the ground due to variations in the two-dimensional or three-dimensional effect during the measurements could be a limitation for the use of the methodology.

Finally, the approach of this work is limited in walls of depth of less than 3 m. Therefore, there are limitations of using this methodology in those basement walls that do not meet these deep conditions. Future research studies could be focused on the feasibility of analysing case studies more deeply.

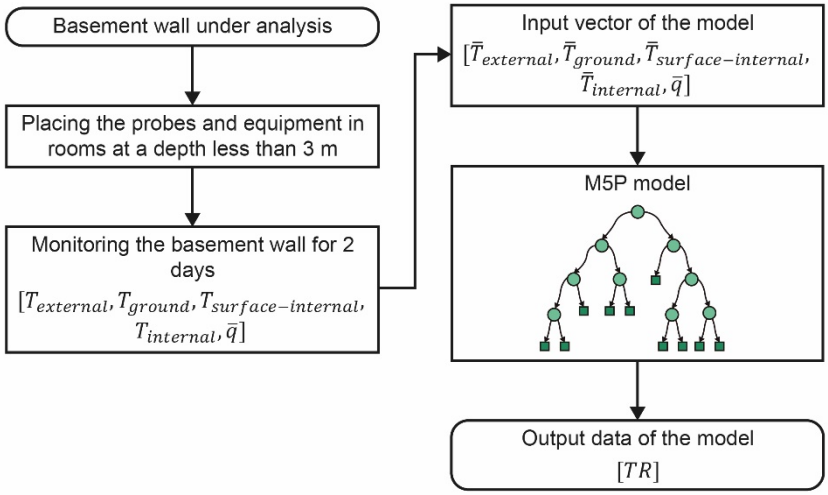

Figure 16. Steps to estimate the thermal resistance of a basement wall.

4. Conclusions

This paper presents a methodology to estimate the thermal resistance of basement walls. Such methodology consists in measuring easily measurable variables (internal air temperature, external air temperature, ground temperature, internal surface temperature, and heat flux) which, together with the use of regression models, allow the thermal resistance to be estimated. Based on the results obtained, the authors of this paper conclude the following:

- The use of the methodology was analysed under controlled conditions. For this purpose, a test model of a calibrated hot-box was designed to simulate the behaviour of the samples in contact with the ground. Such calibrated hot-box could be therefore applied to greater scales to monitor different typologies of basement walls under controlled conditions. Also, the monitoring of basement walls under warm environmental conditions could be analysed. In this way, the ground was in the cold chamber, but it could be in the hot chamber as well. The analysis of the variables of temperature recorded in tests showed that the time required to stabilize the temperature value of the ground was 60 hours. Moreover, this analysis allowed to check that there were isotherms in the ground temperature (i.e., similar to real buildings). Regarding the analysis of the regression models of this phase, the performance obtained by the algorithms was quite adjusted in the time windows considered. In this way, a slight better performance was found for time windows greater than 0.5 days.
- The use of the methodology in actual case studies was analysed. The regression models were generated by using a dataset of 10,579 simulated tests, and they were applied to two actual case studies. In this case, the regression models had different performances. The tree models had a better adjustment than the observations of the training and testing subsets (determination coefficient between 98.81 and 99.86%), whereas multilayer perceptron models had a lower degree of adjustment (a determination coefficient between 90.09 and 97.03%). Also, the error parameters of the estimations of the multilayer perceptrons had increases greater than 155.56% with respect to the tree models. This difference of the performances obtained in the test with the hot-box was due to the great variety of case studies included in the simulations. There was a total of 71 typologies of basement walls, whereas it was only one sample in the hot-box. In addition, the use of time windows of 2 days obtained the best results. The use of the regression models developed with the monitored data in two actual case studies was also analysed. The estimations of the models were accurate with M5 Prime (with differences lower than 0.04 m²K/W), whereas random forests and multilayer perceptrons did not made adequate estimations.

To conclude, the results of this research could be useful for engineers and architects to characterize the performance of buildings with basement walls. On the one hand, the application of the calculation procedures of ISO 13370 would be easier. On the other hand, the energy simulations of the buildings could be optimized by knowing accurately the performance of the envelope, thereby ensuring the proposal of measures to reduce the energy consumption of buildings as well as to achieve the objectives proposed for 2050 (a low-carbon economy). The international aspect of this study

is worth noting because building typologies with inhabitable rooms in contact with the ground are common in various countries, as the case studies of this paper (typologies of basement walls).

Acknowledgements

This work was partially supported by the Spanish Ministry of Science, Innovation and Universities (Code 00064742/ITC-20133094), funded by CDTI (Centro para el Desarrollo Tecnológico e Industrial) under the FEDER-Innterconecta Program, and co-financed with European Union Regional Development Fund. Also, was partially supported by Spanish Ministry of Economy, Industry and Competitiveness (Code BIA 2017-85657-R). The authors would like to acknowledge Own Research Plan of the University of Seville for financing the mobility of David Bienvenido-Huertas and Juan Moyano at the University of A Coruña. Moreover, authors would like to thank Cristian San Millán Parrón and María José Recarey Buño for their help in conducting this research.

References

[1] European Environment Agency, Final energy consumption by sector and fuel (2016), Copenhagen, Denmark, 2018. http://www.eea.europa.eu/data-and-maps/indicators/final-energy-consumption-by-sector-9/assessment-1 (accessed March 9, 2017).
[2] European Commission, Action Plan for Energy Efficiency: Realising the Potential, Brussels, Belgium, 2006.
[3] European Commission, Directive 2002/91/EC of the European Parliament and of the Council of 16 December 2002 on the energy performance of buildings, Brussels, Belgium, 2002.
[4] European Union, Directive 2010/31/EU of the European Parliament and of the Council of 19 May 2010 on the Energy Performance of Buildings, Brussels, Belgium, 2010.
[5] N.A. Kurekci, Determination of optimum insulation thickness for building walls by using heating and cooling degree-day values of all Turkey's provincial centers, Energy Build. 118 (2016) 197–213. doi:10.1016/j.enbuild.2016.03.004.
[6] A. Pérez-Fargallo, C. Rubio-Bellido, J.A. Pulido-Arcas, F. Javier Guevara-García, Fuel Poverty Potential Risk Index in the context of climate change in Chile, Energy Policy. 113 (2018) 157–170. doi:10.1016/j.enpol.2017.10.054.
[7] C. Liddell, C. Morris, H. Thomson, C. Guiney, Excess winter deaths in 30 European countries 1980–2013: a critical review of methods, J. Public Health (Bangkok). 38 (2016) 806–814.
[8] European Commission, A Roadmap for moving to a competitive low carbon economy in 2050, Brussels, Belgium, 2011.
[9] S.W. Rees, M.H. Adjali, Z. Zhou, M. Davies, H.R. Thomas, Ground heat transfer effects on the thermal performance of earth-contact structures, Renew. Sustain. Energy Rev. 4 (2000) 213–265. doi:10.1016/S1364-0321(99)00018-0.
[10] T.P. Bligh, P. Shipp, G. Meixel, Energy comparisons and where to insulate earth-sheltered buildings and basements, Energy. 5 (1980) 451–465. doi:10.1016/0360-5442(80)90020-1.
[11] J. Carmody, R. Sterling, Design considerations for underground buildings, Undergr. Sp. 8.5–6 (1984) 352–362.
[12] F.R. Mazarrón, J. Cid-Falceto, I. Cañas, Ground thermal inertia for energy efficient building design: A case study on food industry, Energies. 5 (2012) 227–242. doi:10.3390/en5020227.
[13] A.A. Al-Temeemi, D.J. Harris, A guideline for assessing the suitability of earth-sheltered mass-housing in hot-arid climates, Energy Build. 36 (2004) 251–260. doi:10.1016/j.enbuild.2003.12.005.
[14] A.J. Anselm, Passive annual heat storage principles in earth sheltered housing, a supplementary energy saving system in residential housing, Energy Build. 40 (2008) 1214–1219. doi:10.1016/j.enbuild.2007.11.002.
[15] F. Wang, Y. Liu, Thermal environment of the courtyard style cave dwelling in winter, Energy Build. 34 (2002) 985–1001. doi:10.1016/S0378-7788(01)00145-1.
[16] M.H. Adjali, M. Davies, J. Littler, Review paper: Earth-contact heat flows: Review and application of design guidance predictions, Build. Serv. Eng. Res. Technol. 19 (1998) 111–121. doi:10.1177/014362449801900301.
[17] J.A. Clarke, T.W. Maver, Advanced design tools for energy conscious building design: Development and dissemination, Build. Environ. 26 (1991) 25–34. doi:10.1016/0360-1323(91)90036-B.
[18] R. Kumar, S. Sachdeva, S.C. Kaushik, Dynamic earth-contact building: A sustainable low-energy technology, Build. Environ. 42 (2007) 2450–2460. doi:10.1016/j.buildenv.2006.05.002.
[19] U.T. Aksoy, M. Inalli, Impacts of some building passive design parameters on heating demand for a cold region, Build. Environ. 41 (2006) 1742–1754. doi:10.1016/j.buildenv.2005.07.011.
[20] A. Invidiata, M. Lavagna, E. Ghisi, Selecting design strategies using multi-criteria decision making to improve the sustainability of buildings, Build. Environ. 139 (2018) 58–68. doi:10.1016/j.buildenv.2018.04.041.
[21] N. Bhikhoo, A. Hashemi, H. Cruickshank, Improving thermal comfort of low-income housing in Thailand through passive design strategies, Sustain. 9 (2017) 1–23. doi:10.3390/su9081440.
[22] J. Ge, J. Wu, S. Chen, J. Wu, Energy efficiency optimization strategies for university research buildings with hot summer and cold winter climate of China based on the adaptive thermal comfort, J. Build. Eng. 18 (2018) 321–330. doi:10.1016/j.jobe.2018.03.022.
[23] J. Yuan, C. Farnham, K. Emura, Optimal combination of thermal resistance of insulation materials and primary fuel sources for six climate zones of Japan, Energy Build. 153 (2017) 403–411. doi:10.1016/j.enbuild.2017.08.039.

[24] J. Ramalho de Freitas, E. Grala da Cunha, Thermal bridges modeling in South Brazil climate: Three different approaches, Energy Build. 169 (2018) 271–282. doi:10.1016/j.enbuild.2018.03.044.
[25] H. Ge, V.R. McClung, S. Zhang, Impact of balcony thermal bridges on the overall thermal performance of multi-unit residential buildings: A case study, Energy Build. 60 (2013) 163–173. doi:10.1016/j.enbuild.2013.01.004.
[26] C. Filippín, S. Flores Larsen, Comportamiento termico de invierno de una vivienda convencional en condiciones reales de uso, Av. En Energías Renov. y Medio Ambient. 9 (2005) 67–72.
[27] W. Bustamante, A. Bobadilla, B. Navarrete, G. Saelzer, S. Vidal, Uso eficiente de la energía en edificios habitacionales. Mejoramiento térmico de muros de albañilería de ladrillos cerámicos. El caso de Chile, Rev. La Construcción. 4 (2005) 5–12.
[28] D. Bienvenido-Huertas, J.A.F. Quiñones, J. Moyano, C.E. Rodríguez-Jiménez, Patents Analysis of Thermal Bridges in Slab Fronts and Their Effect on Energy Demand, Energies. 11 (2018) 2222. doi:10.3390/en11092222.
[29] C. Rubio-Bellido, A. Perez-Fargallo, J.A. Pulido-Arcas, Optimization of annual energy demand in office buildings under the influence of climate change in Chile, Energy. 114 (2016) 569–585. doi:10.1016/j.energy.2016.08.021.
[30] M. Teni, K. Čulo, H. Krstić, Renovation of Public Buildings towards nZEB: A Case Study of a Nursing Home, Buildings. 9 (2019) 153. doi:10.3390/buildings9070153.
[31] I. Ballarini, V. Corrado, F. Madonna, S. Paduos, F. Ravasio, Energy refurbishment of the Italian residential building stock: energy and cost analysis through the application of the building typology, Energy Policy. 105 (2017) 148–160. doi:10.1016/j.enpol.2017.02.026.
[32] R. Adhikari, E. Lucchi, V. Pracchi, Experimental measurements on thermal transmittance of the opaque vertical walls in the historical buildings, in: PLEA2012 Conf. Oppor. Limits Needs Towar. an Environ. Responsible Archit., 2012.
[33] M. Giuliani, G.P. Henze, A.R. Florita, Modelling and calibration of a high-mass historic building for reducing the prebound effect in energy assessment, Energy Build. 116 (2016) 434–448. doi:10.1016/j.enbuild.2016.01.034.
[34] C. Rubio-Bellido, A. Pérez-Fargallo, J.A. Pulido-Arcas, M. Trebilcock, Application of adaptive comfort behaviors in Chilean social housing standards under the influence of climate change, Build. Simul. 10 (2017). doi:10.1007/s12273-017-0385-9.
[35] A. Antonyová, A. Korjenic, P. Antony, S. Korjenic, E. Pavlušová, M. Pavluš, T. Bednar, Hygrothermal properties of building envelopes: Reliability of the effectiveness of energy saving, Energy Build. 57 (2013) 187–192. doi:10.1016/j.enbuild.2012.11.013.
[36] M. de Luxán García de Diego, G. Gómez Muñoz, E. Román López, Towards new energy accounting in residential building, Inf. La Construcción. 67 (2015) 1–10. doi:10.3989/ic.14.059.
[37] D. Bienvenido-Huertas, J. Moyano, D. Marín, R. Fresco-Contreras, Review of in situ methods for assessing the thermal transmittance of walls, Renew. Sustain. Energy Rev. 102 (2019) 356–371. doi:10.1016/j.rser.2018.12.016.
[38] International Organization for Standardization, ISO 6946:2007 - Building components and building elements - Thermal resistance and thermal transmittance - Calculation method, Geneva, Switzerland, 2007.
[39] G. Ficco, F. Iannetta, E. Ianniello, F.R. D'Ambrosio Alfano, M. Dell'Isola, U-value in situ measurement for energy diagnosis of existing buildings, Energy Build. 104 (2015) 108–121. doi:10.1016/j.enbuild.2015.06.071.
[40] I. Ballarini, S.P. Corgnati, V. Corrado, Use of reference buildings to assess the energy saving potentials of the residential building stock: The experience of TABULA project, Energy Policy. 68 (2014) 273–284. doi:10.1016/j.enpol.2014.01.027.
[41] G. Litti, S. Khoshdel, A. Audenaert, J. Braet, Hygrothermal performance evaluation of traditional brick masonry in historic buildings, Energy Build. 105 (2015) 393–411. doi:10.1016/j.enbuild.2015.07.049.
[42] I.N. Grubeša, M. Teni, H. Krstić, M. Vračević, Influence of freeze/thaw cycles on mechanical and thermal properties of masonry wall and masonry wall materials, Energies. 12 (2019) 1–11. doi:10.3390/en12081464.
[43] International Organization for Standardization, ISO 9869-1:2014 - Thermal insulation - Building elements - In situ measurement of thermal resistance and thermal transmittance. Part 1: Heat flow meter method, Geneva, Switzerland, 2014.
[44] P.G. Cesaratto, M. De Carli, S. Marinetti, Effect of different parameters on the in situ thermal conductance evaluation, Energy Build. 43 (2011) 1792–1801. doi:10.1016/j.enbuild.2011.03.021.
[45] G. Desogus, S. Mura, R. Ricciu, Comparing different approaches to in situ measurement of building components thermal resistance, Energy Build. 43 (2011) 2613–2620. doi:10.1016/j.enbuild.2011.05.025.
[46] H. Trethowen, Measurement errors with surface-mounted heat flux sensors, Build. Environ. 21 (1986) 41–56. doi:10.1016/0360-1323(86)90007-7.
[47] X. Meng, B. Yan, Y. Gao, J. Wang, W. Zhang, E. Long, Factors affecting the in situ measurement accuracy of the wall heat transfer coefficient using the heat flow meter method, Energy Build. 86 (2015) 754–765. doi:10.1016/j.enbuild.2014.11.005.
[48] A. Ahmad, M. Maslehuddin, L.M. Al-Hadhrami, In situ measurement of thermal transmittance and thermal resistance of hollow reinforced precast concrete walls, Energy Build. 84 (2014) 132–141. doi:10.1016/j.enbuild.2014.07.048.
[49] I. Nardi, E. Lucchi, T. de Rubeis, D. Ambrosini, Quantification of heat energy losses through the building envelope: A state-of-the-art analysis with critical and comprehensive review on infrared thermography, Build. Environ. 146 (2018) 190–205. doi:10.1016/j.buildenv.2018.09.050.
[50] D. Bienvenido-Huertas, J. Bermúdez, J.J. Moyano, D. Marín, Influence of ICHTC correlations on the thermal characterization of façades using the quantitative internal infrared thermography method, Build. Environ. 149 (2019) 512–525. doi:10.1016/j.buildenv.2018.12.056.

[51] D. Bienvenido-Huertas, J. Bermúdez, J. Moyano, D. Marín, Comparison of quantitative IRT to estimate U-value using different approximations of ECHTC in multi-leaf walls, Energy Build. 184 (2019) 99–113. doi:10.1016/j.enbuild.2018.11.028.
[52] M. Gaši, B. Milovanović, S. Gumbarević, M. Gaši, B. Milovanović, S. Gumbarević, Comparison of Infrared Thermography and Heat Flux Method for Dynamic Thermal Transmittance Determination, Buildings. 9 (2019) 132. doi:10.3390/buildings9050132.
[53] S.-H. Kim, J.-H. Lee, J.-H. Kim, S.-H. Yoo, H.-G. Jeong, The Feasibility of Improving the Accuracy of In Situ Measurements in the Air-Surface Temperature Ratio Method, Energies. 11 (2018) 1–18. doi:10.3390/en11071885.
[54] R. Albatici, A.M. Tonelli, M. Chiogna, A comprehensive experimental approach for the validation of quantitative infrared thermography in the evaluation of building thermal transmittance, Appl. Energy. 141 (2015) 218–228. doi:10.1016/j.apenergy.2014.12.035.
[55] B. Tejedor, M. Casals, M. Gangolells, X. Roca, Quantitative internal infrared thermography for determining in-situ thermal behaviour of façades, Energy Build. 151 (2017) 187–197. doi:10.1016/j.enbuild.2017.06.040.
[56] S. Zoras, A review of building earth-contact heat transfer, Adv. Build. Energy Res. 3 (2009) 289–314. doi:10.3763/aber.2009.0312.
[57] International Organization for Standardization, ISO 13370:2017 - Thermal performance of buildings - Heat transfer via the ground - Calculation methods, 2017.
[58] M. Rotilio, F. Cucchiella, P. De Berardinis, V. Stornelli, Thermal Transmittance Measurements of the Historical Masonries: Some Case Studies, Energies. 11 (2018) 2987. doi:10.3390/en11112987.
[59] E. Lucchi, Thermal transmittance of historical brick masonries: A comparison among standard data, analytical calculation procedures, and in situ heat flow meter measurements, Energy Build. 134 (2017) 171–184. doi:10.1016/j.enbuild.2016.10.045.
[60] E. Lucchi, Thermal transmittance of historical stone masonries: A comparison among standard, calculated and measured data, Energy Build. 151 (2017) 393–405. doi:10.1016/j.enbuild.2017.07.002.
[61] D. Bienvenido-Huertas, J. Moyano, C.E. Rodríguez-Jiménez, D. Marín, Applying an artificial neural network to assess thermal transmittance in walls by means of the thermometric method, Appl. Energy. 233–234 (2019) 1–14. doi:10.1016/j.apenergy.2018.10.052.
[62] D. Bienvenido-Huertas, C. Rubio-Bellido, J.L. Pérez-Ordóñez, J. Moyano, Optimizing the evaluation of thermal transmittance with the thermometric method using multilayer perceptrons, Energy Build. 198 (2019) 395–411. doi:10.1016/j.enbuild.2019.06.040.
[63] D. Bienvenido-Huertas, C. Rubio-Bellido, J.L. Pérez-Ordóñez, M.J. Oliveira, Automation and optimization of in-situ assessment of wall thermal transmittance using a Random Forest algorithm, Build. Environ. 168 (2020). doi:10.1016/j.buildenv.2019.106479.
[64] J. Prata, N. Simões, A. Tadeu, Heat transfer measurements of a linear thermal bridge in a wooden building corner, Energy Build. 158 (2018) 194–208. doi:10.1016/j.enbuild.2017.09.073.
[65] Y.W. Jeong, T.H. Koh, K.S. Youm, J. Moon, Experimental evaluation of thermal performance and durability of thermally-enhanced concretes, Appl. Sci. 7 (2017). doi:10.3390/app7080811.
[66] H. Kus, E. Özkan, Ö. Göcer, E. Edis, Hot box measurements of pumice aggregate concrete hollow block walls, Constr. Build. Mater. 38 (2013) 837–845. doi:10.1016/j.conbuildmat.2012.09.053.
[67] The Government of Spain, Royal Decree 314/2006. Approving the Spanish Technical Building Code, Madrid, Spain, 2013.
[68] S.S. Haykin, S.S. Haykin, S.S. Haykin, S.S. Haykin, Neural networks and learning machines, Pearson Upper Saddle River, 2009.
[69] A.R. Barron, Universal approximation bounds for superpositions of a sigmoidal function, IEEE Trans. Inf. Theory. 39 (1993) 930–945.
[70] C.M. Bishop, Neural networks for pattern recognition: Oxford University Press, Oxford Uni, New York, 1995.
[71] C. Buratti, L. Barelli, E. Moretti, Application of artificial neural network to predict thermal transmittance of wooden windows, Appl. Energy. 98 (2012) 425–432. doi:10.1016/j.apenergy.2012.04.004.
[72] A. Mitra, A. Majumdar, P.K. Majumdar, D. Bannerjee, Predicting thermal resistance of cotton fabrics by artificial neural network model, Exp. Therm. Fluid Sci. 50 (2013) 172–177. doi:10.1016/j.expthermflusci.2013.06.006.
[73] J.R. Quinlan, others, Learning with continuous classes, in: 5th Aust. Jt. Conf. Artif. Intell., 1992: pp. 343–348.
[74] Y. Wang, I.H. Witten, Induction of model trees for predicting continuous classes. proceedings of the poster papers of the european conference on machine learning, (1997).
[75] L. Breiman, J. Friedman, C.J. Stone, R.A. Olshen, Classification and regression trees, Routledge, 2017.
[76] W. Sun, River ice breakup timing prediction through stacking multi-type model trees, Sci. Total Environ. 644 (2018) 1190–1200. doi:10.1016/j.scitotenv.2018.07.001.
[77] M. Xu, P. Watanachaturaporn, P.K. Varshney, M.K. Arora, Decision tree regression for soft classification of remote sensing data, Remote Sens. Environ. 97 (2005) 322–336. doi:10.1016/j.rse.2005.05.008.
[78] V. Rodriguez-Galiano, M. Sanchez-Castillo, M. Chica-Olmo, M. Chica-Rivas, Machine learning predictive models for mineral prospectivity: An evaluation of neural networks, random forest, regression trees and support vector machines, Ore Geol. Rev. 71 (2015) 804–818. doi:10.1016/j.oregeorev.2015.01.001.
[79] A. Behnood, V. Behnood, M. Modiri Gharehveran, K.E. Alyamac, Prediction of the compressive strength of normal and high-performance concretes using M5P model tree algorithm, Constr. Build. Mater. 142 (2017) 199–207. doi:10.1016/j.conbuildmat.2017.03.061.
[80] L. Lin, Q. Wang, A.W. Sadek, A combined M5P tree and hazard-based duration model for predicting urban

freeway traffic accident durations, Accid. Anal. Prev. 91 (2016) 114–126. doi:10.1016/j.aap.2016.03.001.
[81] D. Azofra, E. Martínez, E. Jiménez, J. Blanco, J.C. Saenz-Díez, Comparison of the influence of biomass, solar-thermal and small hydraulic power on the Spanish electricity prices by means of artificial intelligence techniques, Appl. Energy. 121 (2014) 28–37. doi:10.1016/j.apenergy.2014.01.064.
[82] D. Azofra, E. Jiménez, E. Martínez, J. Blanco, J.C. Saenz-Díez, Wind power merit-order and feed-in-tariffs effect: A variability analysis of the Spanish electricity market, Energy Convers. Manag. 83 (2014) 19–27. doi:10.1016/j.enconman.2014.03.057.
[83] D. Azofra, J.C. Saenz-Díez, E. Martínez, E. Jiménez, J. Blanco, Ex-post economic analysis of photovoltaic power in the Spanish grid: Alternative scenarios, Renew. Energy. 95 (2016) 98–108. doi:10.1016/j.renene.2016.04.005.
[84] F. Pallonetto, M. De Rosa, F. Milano, D.P. Finn, Demand response algorithms for smart-grid ready residential buildings using machine learning models, Appl. Energy. 239 (2019) 1265–1282. doi:10.1016/j.apenergy.2019.02.020.
[85] F. Afsarian, A. Saber, A. Pourzangbar, A.G. Olabi, M.A. Khanmohammadi, Analysis of recycled aggregates effect on energy conservation using M5″ model tree algorithm, Energy. 156 (2018) 264–277. doi:10.1016/j.energy.2018.05.099.
[86] S. Dudoit, J. Fridlyand, T.P. Speed, Comparison of discrimination methods for the classification of tumors using gene expression data, J. Am. Stat. Assoc. 97 (2002) 77–87.
[87] B. Larivière, D. Van Den Poel, Predicting customer retention and profitability by using random forests and regression forests techniques, Expert Syst. Appl. 29 (2005) 472–484. doi:10.1016/j.eswa.2005.04.043.
[88] L. Breiman, Bagging predictors, Mach. Learn. 24 (1996) 123–140.
[89] L. Breiman, Random forests, Mach. Learn. 45 (2001) 5–32. doi:10.1023/A:1010933404324.
[90] D. Assouline, N. Mohajeri, J.L. Scartezzini, Large-scale rooftop solar photovoltaic technical potential estimation using Random Forests, Appl. Energy. 217 (2018) 189–211. doi:10.1016/j.apenergy.2018.02.118.
[91] S. Sinharay, An overview of statistics in education, (2010).
[92] B. Cui, C. Fan, J. Munk, N. Mao, F. Xiao, J. Dong, T. Kuruganti, A hybrid building thermal modeling approach for predicting temperatures in typical, detached, two-story houses, Appl. Energy. 236 (2019) 101–116. doi:10.1016/j.apenergy.2018.11.077.
[93] C.E. Kontokosta, C. Tull, A data-driven predictive model of city-scale energy use in buildings, Appl. Energy. 197 (2017) 303–317. doi:10.1016/j.apenergy.2017.04.005.
[94] A. Ghahramani, J. Pantelic, C. Lindberg, M. Mehl, K. Srinivasan, B. Gilligan, E. Arens, Learning occupants' workplace interactions from wearable and stationary ambient sensing systems, Appl. Energy. 230 (2018) 42–51. doi:10.1016/j.apenergy.2018.08.096.
[95] R. Kohavi, A Study of Cross-Validation and Bootstrap for Accuracy Estimation and Model Selection, in: Int. Jt. Conf. Artif. Intell., 1995. doi:10.1067/mod.2000.109031.
[96] D.E. Rumelhart, G.E. Hinton, R.J. Williams, Learning representations by back-propagating errors, Nature. 323 (1986) 533–536. doi:10.1038/323533a0.
[97] R. Fletcher, Practical methods of optimization, John Wiley&Sons, Chichester - New York - Brisbane - Toronto, United States, 1980.
[98] International Organization for Standardization, ISO 8990:1994 - Thermal insulation - Determination of steady-state thermal transmission properties - Calibrated and guarded hot box, Geneva, Switzerland, 1994.
[99] M. Teni, H. Krstić, P. Kosiński, Review and comparison of current experimental approaches for in-situ measurements of building walls thermal transmittance, Energy Build. 203 (2019) 109417. doi:10.1016/j.enbuild.2019.109417.
[100] H.R. Thomas, S.W. Rees, The thermal performance of ground foor slabs-a full scale in!situ experiment, Build. Environ. 34 (1999) 139–164.
[101] D. Bienvenido-Huertas, C. Rubio-Bellido, J. Pérez-Ordóñez, F. Martínez-Abella, Estimating Adaptive Setpoint Temperatures Using Weather Stations, Energies. 12 (2019) 1197. doi:10.3390/en12071197.
[102] International Organization for Standardization, ISO 10211:2017 - Thermal bridges in building construction - Heat flows and surface temperatures - Detailed calculations, Geneva, Switzerland, 2017.
[103] F. Kurtz, M. Monzón, B. López-Mesa, Energy and acoustics related obsolescence of social housing of Spain's post-war in less favoured urban areas. The case of Zaragoza, Inf. La Construcción. 67 (2015) m021. doi:10.3989/ic.14.062.
[104] S. Domínguez-Amarillo, J.J. Sendra, I. Oteiza, La envolvente térmica de la vivienda social. El caso de Sevilla, 1939 a 1979, Editorial CSIC: Madrid, 2016.
[105] Eduardo Torroja Institute for Construction Science, Constructive elements catalogue of the CTE, 2010.